

From the Center of Experimental Orthopaedics

Saarland University

Director: Prof. Dr. med. Henning Madry

**Combined rAAV-based gene therapy and tissue engineering  
approaches to enhance the molecular mechanisms of  
articular cartilage repair**

*Dissertation for the degree of Doctor of Medicine and Natural Sciences (MD-PhD)*

**Faculty of Medicine**

**SAARLAND UNIVERSITY**

2021

submitted by:

Weikun Meng

born on: 28.05.1990 in Yunnan, P. R. China

## Declaration

I hereby declare that this thesis is my own original work and effort. All experiments, except for those specified, were exclusively performed by me. Except for the publications written by myself listed in the publication list, the data presented here have not been submitted anywhere else for any award. Where other sources of information and help that have been used, they have been indicated and acknowledged.

Homburg, 16.06.2021

*Weikun Meng*

---

Weikun Meng

Tag der Promotion: 10.03.2022

Dekan: Prof. Dr. M. D. Menger

Berichterstatter: Prof. M. Madry  
Prof. L. Prates-Roma  
Prof. M. Amling

# CONTENT

<b>List of Abbreviations</b> .....	<b>1</b>
<b>List of Figures</b> .....	<b>3</b>
<b>List of Tables</b> .....	<b>4</b>
<b>1. ABSTRACT</b> .....	<b>5</b>
<b>2. ZUSAMMENFASSUNG</b> .....	<b>6</b>
<b>3. INTRODUCTION</b> .....	<b>8</b>
<b>3.1. Articular cartilage</b> .....	<b>8</b>
3.1.1. <i>Articular cartilage structure and composition</i> .....	8
3.1.2. <i>Articular cartilage injury and treatment</i> .....	10
<b>3.2. Carbon dots</b> .....	<b>11</b>
3.2.1. <i>Structure and optical properties of carbon dots</i> .....	11
3.2.2. <i>Carbon dots as probes for gene delivery</i> .....	12
<b>3.3. Gene delivery vectors</b> .....	<b>16</b>
3.3.1. <i>Nonviral vectors</i> .....	17
3.3.2. <i>Viral vectors</i> .....	17
3.3.3. <i>rAAV vectors</i> .....	19
<b>3.4. Therapeutic candidate: SOX9</b> .....	<b>20</b>
3.4.1. <i>Functions of SOX9</i> .....	20
3.4.2. <i>Application of SOX9 to enhance chondrogenesis in vitro</i> .....	26
3.4.3. <i>Application of SOX9 to enhance chondrogenesis and cartilage repair in vivo</i> .....	28
<b>3.5. Therapeutic gene: TGF-<math>\beta</math></b> .....	<b>29</b>
3.5.1. <i>Functions of TGF-<math>\beta</math></i> .....	29
3.5.2. <i>Application of TGF-<math>\beta</math> to enhance chondrogenesis in vitro</i> .....	32
3.5.3. <i>Application of TGF-<math>\beta</math> to enhance chondrogenesis and cartilage repair in vivo</i>	

.....	33
3.6. Outlook .....	34
4. HYPOTHESES.....	35
5. MATERIALS .....	36
5.1. Chemicals .....	36
5.2. Solution and buffers .....	37
5.3. Equipment .....	39
5.4. Software.....	39
6. METHODS.....	40
6.1. Study design .....	40
6.2. Preparation of hMSCs.....	40
6.3. Preparation of carbon dots .....	41
6.4. Preparation of rAAV vectors .....	42
6.5. Cy3 labeling.....	43
6.6. Complexation of rAAV vectors with carbon dots and release studies.....	43
6.7. rAAV/carbon dot-mediated gene transfer .....	44
6.8. Analysis of transgene expression.....	44
6.9. Cell viability and proliferation.....	44
6.10. Histology and immunohistochemistry .....	45
6.11. Histomorphometric analyses .....	45
6.12. Statistical analysis.....	45
7. RESULTS .....	46
7.1. Effective rAAV association to carbon dots and release .....	46
7.2. Effective carbon dot-guided, rAAV-mediated reporter <i>lacZ</i> overexpression in hMSCs.....	48
7.3. Effective carbon dot-guided, rAAV-mediated SOX9 and TGF- $\beta$ overexpression in hMSCs .....	52
7.4. Effects of carbon dot-guided, rAAV-mediated SOX9 and TGF- $\beta$	

overexpression on the biological activities in hMSCs.....	54
<b>8. DISCUSSION .....</b>	<b>58</b>
8.1. Carbon dots as effective systems to formulate and release rAAV gene transfer vectors .....	59
8.2. Effects of rAAV/carbon dot application on the viability of hMSCs .....	59
8.3. CD-2 as an optimal carbon dot systems to deliver therapeutic (SOX9, TGF- $\beta$ ) rAAV vectors .....	60
8.4. Limitations and strengths .....	62
8.5. Clinical implications .....	63
<b>9. CONCLUSIONS .....</b>	<b>64</b>
<b>10. REFERENCES .....</b>	<b>65</b>
<b>11. PUBLICATIONS AND PRESENTATIONS.....</b>	<b>85</b>
11.1. Publications .....	85
11.2. Poster presentations.....	86
<b>12. ACKNOWLEDGEMENTS .....</b>	<b>87</b>

## List of Abbreviations

AAV	adeno-associated virus
$\beta$ -gal	$\beta$ -galactosidase
bp	base-pair
CD-1 to CD-4	carbon dot-1 to carbon dot-4
cDNA	complementary deoxyribonucleic acid
Da	Dalton
DMEM	Dulbecco's modified Eagle's medium
DNA	deoxyribonucleic acid
ELISA	enzyme-linked immunosorbent assay
FLAG	tag sequence
HEPES	4-(2-hydroxyethyl)-1-piperazineethanesulfonic acid
hMSCs	human bone marrow-derived mesenchymal stromal cells
IL-1 $\beta$	interleukin 1 beta
kb	kilobase
<i>lacZ</i>	<i>E. coli</i> $\beta$ -galactosidase
microRNA	micro-ribonucleic acid
MOI	multiplicity of infection
mRNA	messenger ribonucleic acid
MW	molecular weight
OA	osteoarthritis
OD	optical density
PBS	phosphate-buffered saline
PCR	polymerase chain reaction
PEG	poly(ethylene glycol)
PEI	polyethylenimine
rAAV	recombinant adeno-associated viral vector
RNA	ribonucleic acid
SD	standard deviation

rTGF- $\beta$	recombinant transforming growth factor beta
SMAD	small mothers against decapentaplegic
SOX9	sex-determining region Y-type high mobility group box 9
TGF- $\beta$	transforming growth factor beta
TNF- $\alpha$	tumor necrosis factor alpha

## List of Figures

<b>Figure 1.</b> Collagen fiber arrangements in cartilage showing the zonal structure of the articular cartilage .....	9
<b>Figure 2.</b> Gene delivery and real-time monitoring of cellular trafficking utilizing carbon dot-polyethylenimine/gold-polyethylenimine/plasmid DNA assembly of nanohybrids ....	12
<b>Figure 3.</b> Formation of carbon dot-polyethylenimine and carbon dot-polyethylenimine/plasmid DNA complexes .....	13
<b>Figure 4.</b> Carbon dot/DNA synthesis .....	14
<b>Figure 5.</b> Synthesis of folate-conjugated reducible PEI-passivated carbon dot/small interfering RNA nanoagents .....	15
<b>Figure 6.</b> Formation of carbon dot/plasmids .....	16
<b>Figure 7.</b> Preparation of rAAV gene transfer vectors.....	19
<b>Figure 8.</b> Sequential effects of SOX9 on chondrogenesis.....	21
<b>Figure 9.</b> Signaling pathways of TGF- $\beta$ and Wnt involved in joint pathophysiology .....	30
<b>Figure 10.</b> Structural features of the various carbon dots tested in the studies .....	41
<b>Figure 11.</b> Complexation and release of rAAV from the carbon dots .....	47
<b>Figure 12.</b> Detection of reporter ( <i>lacZ</i> ) overexpression in hMSCs transduced with the rAAV/carbon dot systems .....	49
<b>Figure 13.</b> Cell viability in hMSCs transduced with the rAAV/carbon dot systems .....	51
<b>Figure 14.</b> Detection of therapeutic (SOX9, TGF- $\beta$ ) gene overexpression in hMSCs transduced with rAAV/CD-2 .....	53
<b>Figure 15.</b> Biological activities in hMSCs transduced with rAAV/CD-2.....	56

## List of Tables

<b>Table 1.</b> Gene transfer vectors .....	18
<b>Table 2.</b> Positive SOX9 regulation.....	23
<b>Table 3.</b> Negative SOX9 regulation .....	26
<b>Table 4.</b> Application of SOX9 to enhance chondrogenesis <i>in vitro</i> .....	27
<b>Table 5.</b> Application of SOX9 to enhance chondrogenesis and cartilage repair <i>in vivo</i> ..	28
<b>Table 6.</b> Application of TGF- $\beta$ to enhance chondrogenesis <i>in vitro</i> .....	33
<b>Table 7.</b> Application of TGF- $\beta$ to enhance chondrogenesis and cartilage repair <i>in vivo</i> .	34
<b>Table 8.</b> Chemicals used in the studies .....	36
<b>Table 9.</b> Solutions and buffers used in the studies .....	37
<b>Table 10.</b> Equipment used in the studies.....	39
<b>Table 11.</b> Software used in the studies.....	39
<b>Table 12.</b> Characteristics of the carbon dots (CD-1 to CD-4) employed in the studies...	42
<b>Table 13.</b> Histomorphometric analyses in hMSCs transduced with rAAV/CD-2 .....	54

## 1. ABSTRACT

Articular cartilage defects do not regenerate. Scaffold-assisted gene therapy is a highly promising novel approach for cartilage repair. Carbon dots, a class of carbon-dominated nanomaterials, are spherical carbonaceous nanomaterials of small sizes exhibiting water dispersibility, chemical stability, photoluminescence properties, and photostability.

Here, the potential benefits of using carbon dots to deliver genes coding for the chondroreparative sex-determining region Y-type high-mobility group box 9 (SOX9) transcription factor and transforming growth factor beta (TGF- $\beta$ ) via the clinically adapted recombinant adeno-associated virus (rAAV) vectors were investigated as a means to stimulate chondrogenic processes in human bone marrow-derived mesenchymal stromal cells (hMSCs) *versus* control (reporter rAAV-*lacZ* vector) application. hMSCs naturally repopulate cartilage defects but tend to lose their chondrogenic potential over time. Carbon dot-guided genetic modification of hMSCs may rejuvenate these cells in the defects either upon administration of carbon dot/rAAV composites *in vivo* or by implantation of hMSCs genetically modified by the composites.

Four carbon dots were tested to identify an optimal compound (CD-1: citric acid, pentaethylenehexamine; CD-2: citric acid, poly(ethylene glycol) (PEG) monomethyl ether MW 550 Da, *N,N*-dimethylethylenediamine; CD-3: citric acid, branched poly(ethylenimine) MW 600 Da, PEG monomethyl ether MW 2 kDa; CD-4: citric acid, branched poly(ethylenimine) MW 600 Da). All were capable of formulating and releasing rAAV-*lacZ* for an effective modification of hMSCs. Among them, CD-2 was optimal to effectively and safely deliver rAAV for at least 10 days, the longest time point examined. Administration of therapeutic (SOX9, TGF- $\beta$ ) rAAV vectors via CD-2 led to an effective overexpression of these genes in hMSCs, enhancing cell proliferation (TGF- $\beta$ ) and matrix deposition (glycosaminoglycans, type-II collagen) (SOX9, TGF- $\beta$ ) for at least 21 days relative to control treatments (CD-2 formulating rAAV-*lacZ* or lacking rAAV), while restricting undesirable type-I and -X collagen deposition (SOX9, TGF- $\beta$ ). These results show the potential of carbon dot-guided rAAV modification of hMSCs as a minimally invasive system for translational strategies aiming at enhancing cartilage repair.

## 2. ZUSAMMENFASSUNG

Defekte des hyalinen Gelenknorpels regenerieren nicht. Die gerüstgestützte Gentherapie ist ein vielversprechender neuer Ansatz für die Knorpelreparatur. *Carbon-Dots* (Kohlenstoff-Punkte), eine Klasse kohlenstoffdominierter Nanomaterialien, sind kugelförmige kohlenstoffhaltige Nanomaterialien kleiner Größe, die Wasserdispergierbarkeit, chemische Stabilität, Photolumineszenz sowie und Photostabilität aufweisen.

In der vorliegenden Arbeit wurden die potenziellen Vorteile der Verwendung von *Carbon-Dots* zur Bereitstellung von Genvektoren auf Basis der klinisch-adaptiven rekombinanten adeno-assoziierten viralen (rAAV) Vektoren für den chondrogenen Transkriptionsfaktor SOX9 (geschlechtsbestimmende Region Y-Typ-Hochmobilitätsgruppenbox 9) und den transformierenden Wachstumsfaktor beta (TGF- $\beta$ ) zur Stimulierung chondrogener Prozesse in aus humanem Knochenmark gewonnenen mesenchymalen Stromazellen (hMSCs) im Vergleich zur Kontrollanwendung (Reporter-rAAV-*lacZ*-Vektor) untersucht. Obwohl hMSCs auf natürliche Weise Knorpeldefekte besiedeln, neigen sie dazu, ihr chondrogenes Potenzial im Laufe der Zeit zu verlieren. Eine durch *Carbon-Dots* gesteuerte genetische Modifikation von hMSCs kann diese Zellen in den Defekten entweder durch die Verabreichung von *Carbon-Dots*/rAAV-Kompositen *in vivo* oder durch Implantation von durch diese Komposite genetisch modifizierter hMSCs phänotypisch modulieren.

Vier Arten von *Carbon-Dots* wurden analysiert, um eine optimale Verbindung zu identifizieren [CD-1: Zitronensäure, Pentaethylenhexamin; CD-2: Zitronensäure, Polyethylenglykolmonomethylether (Molekülmasse  $M = 550$  Da), N, N-Dimethylethylendiamin; CD-3: Zitronensäure, verzweigtes Polyethylenimin, ( $M = 600$  Da), Polyethylenglykolmonomethylether ( $M = 2000$  Da); CD-4: Zitronensäure, verzweigtes Polyethylenimin ( $M = 600$  Da)]. Alle Komponenten waren in der Lage, rAAV-*lacZ* für eine wirksame genetische Modifikation von hMSCs zu formulieren und freizusetzen. Unter diesen war CD-2 optimal, um rAAV für mindestens 10 Tage, den längsten untersuchten Zeitpunkt, effektiv und sicher freizusetzen. Die CD-2-vermittelte

Verabreichung der therapeutischen SOX9- oder TGF- $\beta$ -rAAV-Vektoren führte zu einer wirksamen Überexpression dieser Gene in hMSCs, wodurch die Zellproliferation (TGF- $\beta$ ) und die Matrixdeposition (Glykosaminoglykane, Typ-II-Kollagen) (jeweils nach SOX9 und TGF- $\beta$ -Therapie) für mindestens 21 Tage im Vergleich zu Kontrollbehandlungen (CD-2, ohne oder mit rAAV-*lacZ* formuliert) verstärkt wurde, während eine unerwünschte Typ-I- und Typ-X-Kollagenproduktion jeweils nach SOX9 und TGF- $\beta$ -Therapie reduziert ist. Diese Ergebnisse zeigen das Potenzial einer durch *Carbon-Dots* gesteuerten rAAV-Modifikation von hMSCs als minimalinvasives System für translationale Strategien zur Verbesserung der klinischen Knorpelreparatur.

## 3. INTRODUCTION

### 3.1. Articular cartilage

Hyaline articular cartilage is the highly specialized dense connective tissue covering all synovial joints. Its primary function is to provide articulation with a smooth, lubricated surface and to facilitate the transfer of loads with a low coefficient of friction. Deprived of blood vessels, lymphatics, and nerves, articular cartilage is subject to a harsh biomechanical environment. Articular cartilage, most importantly, has a limited potential for intrinsic healing and repair. The preservation and health of articular cartilage are paramount to joint health in this respect. The special and intricate structure of articular cartilage makes it extremely difficult for patients and healthcare workers to treat and repair or restore defects. Articular cartilage preservation is highly dependent on preserving its organized architecture.

#### *3.1.1. Articular cartilage structure and composition*

Articular cartilage consists of a highly organized dense extracellular matrix with a sparse distribution of a highly specialized single cell type cell called the chondrocyte. The extracellular matrix consists primarily of water, collagen, and proteoglycans, with smaller proportions of other non-collagenous proteins and glycoproteins (Buckwalter and Mankin, 1997, 1998; Newman, 1998). These components together help to preserve water within the extracellular matrix, which is critical for maintaining its unique mechanical properties. To better understand and manage the articular cartilage injury, it is vital to understand the natural function and structure of the articular cartilage. From the articular surface to the subchondral bone, the macrostructure of articular cartilage is best described in four distinct zones: superficial, transitional, deep, and calcified zones (**Figure 1**).

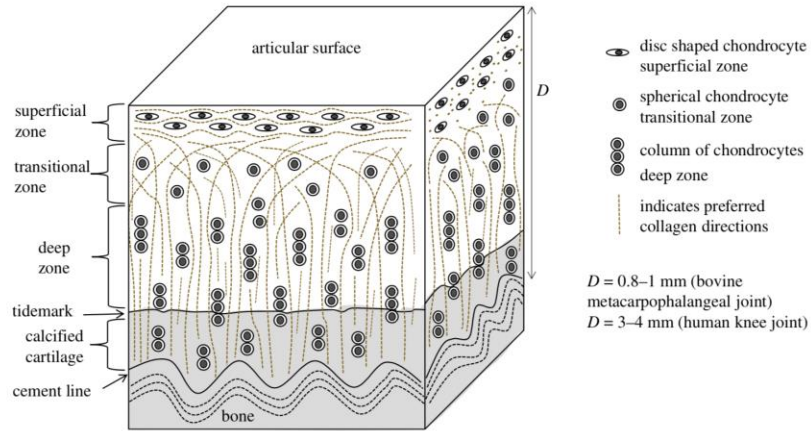


**Figure 1.** Collagen fiber arrangements in cartilage showing the zonal structure of the articular cartilage. Image from (Mansfield et al., 2019).

The superficial zone (tangential, gliding surface) locates the outermost articular surface. It makes up approximately 10% to 20% of articular cartilage thickness. The collagen fibrils (primarily type-II and -IX collagen) are oriented parallel to the surface within the superficial zone. Chondrocytes are flattened; the water content is at its highest; proteoglycan volume is at its lowest. With those unique characteristics, this zone is responsible for most of the cartilage's tensile properties, allowing it to withstand the articulation-imposed shear, tensile, and compressive forces.

The transitional (middle) zone is immediately deep into the superficial zone. The transitional zone accounts for 40-60% of the total volume of cartilage. In this zone, the larger diameter collagen fibers with less organized obliquely, and the chondrocytes are rounder and at low density. The transitional zone is characterized by an anatomic and functional bridge between the tangential and deep zones, its functions as the first line to resist to compressive forces.

The deep zone is below the transitional zone. It represents approximately 30% of the total articular cartilage volume. The deep zone is characterized by the largest diameter collagen fibers oriented perpendicular to the articular surface. In this zone, the chondrocytes appear spherical and are typically arranged in columnar orientation, parallel to the collagen fibers and perpendicular to the joint line. The concentration of the

water content is the lowest and proteoglycan is the highest. With those unique properties, the deep zone is responsible for providing the greatest resistance to compressive forces.

The deepest zone of the articular cartilage is the calcified zone; the tidemark, a complex three-dimensional structure with a distinct microanatomical trilaminar appearance, divides calcified cartilage from the articular cartilage. Collagen fibrils (mainly type-II collagen) cross the tidemark, resulting in a rather strong link between these two zones. This deepest layer plays a transitional role in hyaline cartilage to the subchondral bone. In this zone, the collagen fibrils are arranged perpendicular to the articular cartilage. The chondrocytes are small, scarce, and hypertrophic. This stiff zone is likely to obstruct nutrient transport from the underlying bone, making the articular cartilage dependent on the nutritional support of synovial fluid.

### *3.1.2. Articular cartilage injury and treatment*

Articular cartilage injury from trauma or degeneration represents a significant cause of morbidity with a frequent occurrence in synovial joints. Treatment of cartilage injuries is challenging because the articular cartilage is a highly specialized white connective tissue without blood supply, innervation, and lymphatic system. Joint pain, tissue swelling, and mechanical symptoms (locking, trapping, crepitus) often occur in patients with cartilage damage which drive them to seek care to alleviate secondary symptoms of joint disability (Grande et al., 2013). Non-operative therapies aim at managing symptoms using anti-inflammatory medication, viscosupplementation, bracing, orthotics, and activity modification (Buttgereit et al., 2015; Simon and Jackson, 2018). Drilling, abrasion, and microfracture of the subchondral bone provide surgical techniques to stimulate the intrinsic fibrocartilaginous repair process (Gao et al., 2018; Simon and Jackson, 2018; Steadman et al., 2001). At present, autologous chondrocyte implantation, periosteal transfer, and osteochondral autograft or allograft transplantation are commonly used clinical methods for the treatment of cartilage defects (Simon and Jackson, 2018). Many new, attractive strategies employing tissue engineering involve the use of combinations of biomaterial, cells, bioactive factors, and matrices, and synthetic devices.

## 3.2. Carbon dots

Carbon dots, a new class of fluorescent carbon nanoparticles also called carbon quantum dots, were discovered by Xu *et al.* (Xu *et al.*, 2004) after separation and purification of single-walled carbon nanotubes synthesized by arc-discharge methods. Carbon dots, however, have a significant distinction - they are made of carbon, an abundant and typically non-toxic element, which is also one of life's own building blocks. The carbon-based structural features include a good biocompatibility, unique optical properties, low toxicity, aqueous stability, and easy to produce (Baker and Baker, 2010; Li *et al.*, 2012). The carbon composition of the carbon dots offers specific structural and electronic properties that are distinct from other families of nanoparticles. Indeed, in the world of nanoparticle biomedical applications, biocompatibility has been touted as one of the principal benefits of carbon dots. Those basic facts make carbon dots especially appealing for applications that include biological imaging, drug delivery, and gene delivery in many biomedical applications for which toxicity risks pose challenges.

### 3.2.1. Structure and optical properties of carbon dots

In general, carbon dots are nanocrystallites or amorphous nanoparticles knitted up via  $sp^2$  bonding (Kailasa *et al.*, 2019). Depending on the precursor and preparation methods, their height varies from 0.5 to 5 nm. A typical high-resolution transmission electron microscopy study reported that carbon dots show an obvious fringe spacing of  $\sim 0.34$  nm (Kailasa *et al.*, 2019). Interestingly, carbon dots with multiple functional groups, in particular oxygen-related functional groups (carboxyl, hydroxyl), are functionalized during carbonization, imparting excellent water solubility, and sufficient chemically reactive groups for surface passivation and derivatization of different organic, polymeric or biological materials. The unique optical and physicochemical properties of carbon dots can be tuned by their size, shape, heteroatom doping, and surface functional groups. As a result, carbon dots possess various interesting and useful properties such as good water solubility, good material stability, high fluorescence efficiency, nontoxicity, tunability and stability, good biocompatibility, and easy functionalization, enabling them to open up a wide prospect of biomedical use.

### 3.2.2. Carbon dots as probes for gene delivery

In biomedical applications, carbon dot-based nanocarriers gained increased attention due to their biocompatible and physicochemical features. Carbon dots opened avenues for gene delivery applications because of their biocompatibility and of a wide range of surface functional groups. As vehicles for the delivery of negatively charged deoxyribonucleic acid (DNA) fragments, many currently employed gene carriers use positively charged polymeric materials. Kim *et al.* (Kim et al., 2013) revealed the potential of carbon dot-polyethylenimine (PEI)/gold (Au)-PEI/plasmid DNA ternary nanoassemblies as highly efficient hybrid transfecting agents allowing for high cell viability under optimal conditions. This nanoassembly system was found to be very efficient for the non-labeled monitoring of the carrier/plasmid DNA dissociation, providing an effective strategy to study the mechanistic aspects of the delivery of polymer-mediated plasmid DNA (**Figure 2**).

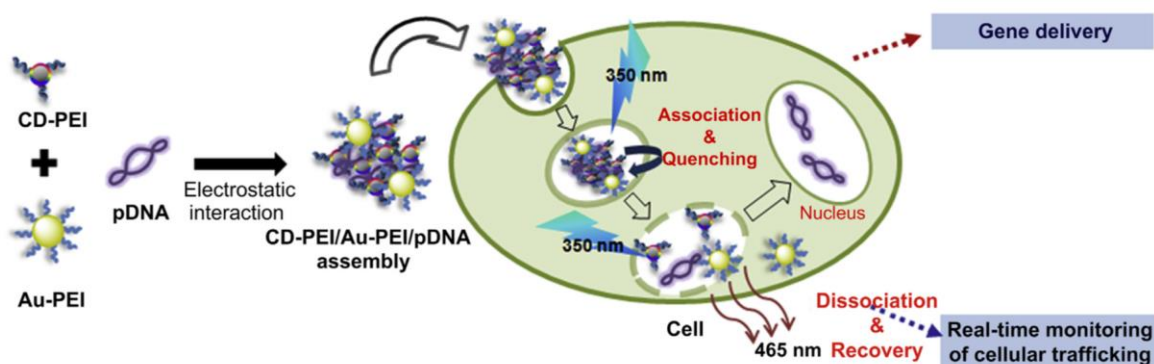


**Figure 2.** Gene delivery and real-time monitoring of cellular trafficking utilizing carbon dot-polyethylenimine/gold-polyethylenimine/plasmid DNA assembly of nanohybrids. Abbreviations: CD, carbon dot; PEI, polyethylenimine; Au, gold; pDNA, plasmid DNA. Image from (Kim et al., 2013).

Liu *et al.* (Liu et al., 2012) successfully constructed functionalized carbon dot-PEI obtained at an appropriate pyrolysis time that exhibited lower toxicity, higher or comparable gene expression of plasmid DNA in African green monkey kidney cells and human hepatocellular liver carcinoma line cells relative to control PEI compound. Interestingly, the carbon dot-PEI internalized into cells displayed tunable fluorescent emission under varying excitation wavelength, supporting the concept of further manipulating carbon dot-PEI in gene delivery and bioimaging (**Figure 3**).

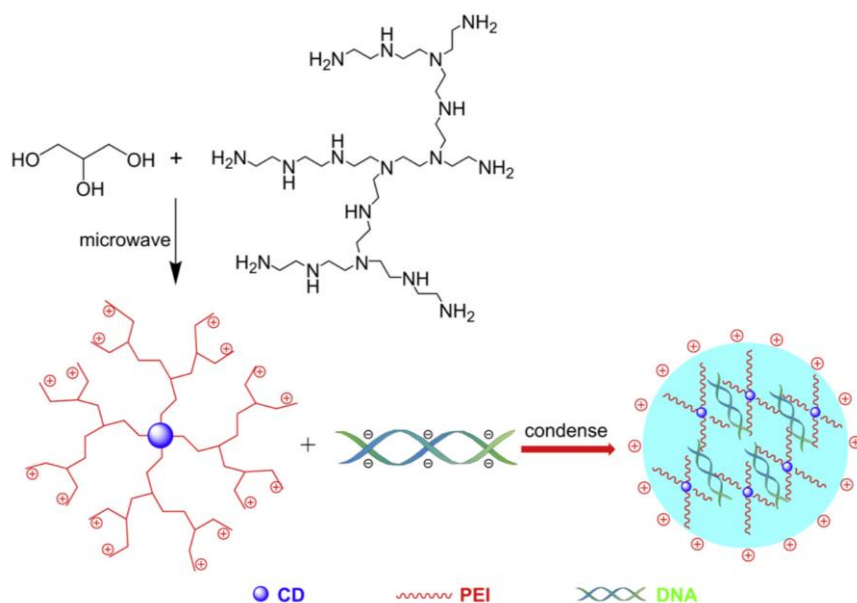


**Figure 3.** Formation of carbon dot-polyethylenimine and carbon dot-polyethylenimine/plasmid DNA complexes. Abbreviations: CD, carbon dot; PEI, polyethylenimine; DNA, deoxyribonucleic acid. Image from (Liu et al., 2012).

Ding *et al.* (Ding et al., 2015) described a green system to produce highly biocompatible carbon dot/DNA using genomic DNA isolated from *E. coli* that can be purified using a simple column centrifugation-based system (**Figure 4**), as a new type of fluorescent vehicle for cell imaging and drug delivery studies.

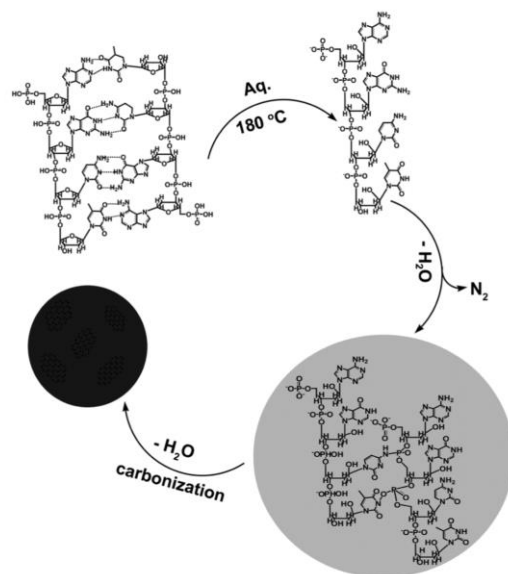


**Figure 4.** Carbon dot/DNA synthesis. Image from (Ding et al., 2015).

Hu *et al.* (Hu et al., 2014) found that branched carbon dot-PEI also exhibit a high biocompatibility and can be applied for gene delivery. Because of their specific nanostructure and photoluminescence properties, multifunctional carbon dot-PEI have a strong potential for bioimaging and gene delivery. Wu *et al.* (Wu et al., 2016) successfully synthesized a novel multifunctional theranostic folate-conjugated reducible PEI-passivated carbon dots carrying a small interfering RNA for imaging-guided lung cancer therapy, i.e. folate-conjugated reducible PEI-passivated carbon dot/small interfering RNA nanoagent (**Figure 5**). The theranostic system absorbed at 360 nm and emitted at 460 nm, the wavelength of blue light. In the diagnostic modality of the theranostic carbon dots, the highest photoluminescent peak appeared at 460 nm and apoptotic cell death occurred in the therapeutic segment.

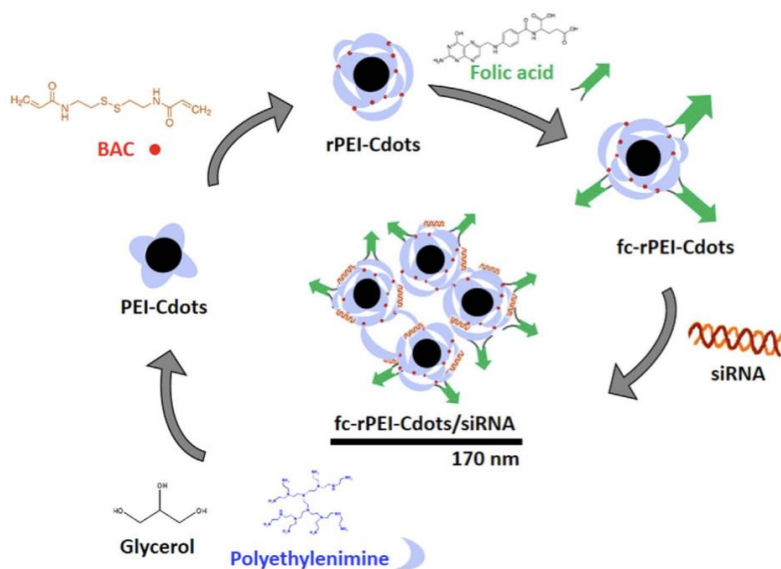


**Figure 5.** Synthesis of folate-conjugated reducible PEI-passivated carbon dot/small interfering RNA nanoagents. Abbreviation: fc-rPEI-Cdots/siRNA, folate-conjugated reducible polyethylenimine-passivated carbon dot/small interfering ribonucleic acid. Image from (Wu et al., 2016).

In another study, Wong *et al.* (Wong et al., 2018) created stimuli-responsive nanoparticles composed of cationic  $\beta$ -cyclodextrin-modified PEI, tetronic polyrotaxane end-capped with adamantane, and carbon dot-Arg-Gly-Asp to package microRNA and plasmid DNA. The self-assembled nanoparticles disassembled at endosomal pH, allowing to release the carbon dots to induce endosomal rupture and render the plasmids available for nuclear transport. Zhou *et al.* (Zhou et al., 2016a) generated carbon dots at high biocompatibility and low toxicity using alginate to deliver a plasmid carrying TGF- $\beta$ 1 in 3T6 cells at high transfection efficiency. Cao *et al.* (Cao et al., 2018) confirmed that carbon dot-mediated delivery of a plasmid carrying SOX9 successfully induced the chondrogenesis of mouse embryonic fibroblasts. Overall, the application of carbon dots holds great promise for nonviral gene transfer, tissue engineering, and bioimaging (**Figure 6**).

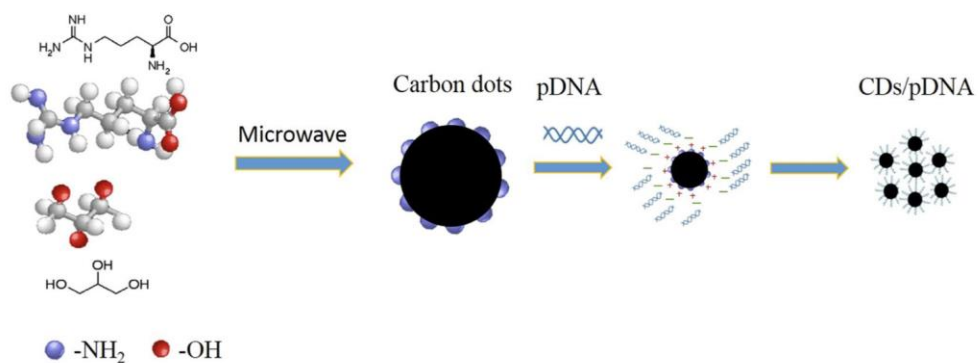


**Figure 6.** Formation of carbon dot/plasmids. Abbreviations: pDNA, plasmid deoxyribonucleic acid; CDs, carbon dots. Image from (Cao et al., 2018).

### 3.3. Gene delivery vectors

Gene delivery focuses on the introduction of foreign or therapeutic gene sequences in a target cell population as a means to treat a specific disease in affected individuals through gene therapy and/or regenerative medicine, based on a prolonged expression of a transgene cassette being delivered compared with the application of the therapeutic product itself with short pharmacological half-life (Rey-Rico and Cucchiarini, 2016a). Nevertheless, the vulnerability of naked DNA to degradation by nucleases present in biological media and the hydrophilic polyanionic nature and large size of DNA molecules prevent passive DNA penetration through the cell membrane (Ibraheem et al., 2014; Nam et al., 2009). Therefore, vectors capable of carrying therapeutic molecules in target cells must be paired with DNA (Ibraheem et al., 2014). Gene delivery vectors currently involved in articular cartilage repair include nonviral vectors (Cucchiarini et al., 2015; Gelse et al., 2008; Goomer et al., 2000) and viral vehicles (Cucchiarini and Madry, 2019; Garza-Veloz et al., 2013; Gelse et al., 2003; Madry et al., 2020a, 2020b; Mbita et al., 2014; Meng et al., 2020; Venkatesan et al., 2020b).

### 3.3.1. Nonviral vectors

Gene delivery via nonviral vectors (transfection) is the incorporation of plasmid DNA alone or complexed with cationic or ionizable lipids (lipoplexes), cationic polymers (polyplexes), or a combination of both (lipopolyplexes) (Rezaee et al., 2016) in a target population (Bono et al., 2020). The use of niosomes (nioplexes) (Alvarez-Rivera et al., 2020), dendrimers (dendriplexes) (Rai et al., 2019), and gold or carbon nanostructures (Sum et al., 2018) are also more recent approaches. Nonviral vectors are generally considered safe carriers as they do not carry the risk of insertional mutagenesis (nonviral vectors are kept in episomal forms) and have low immunogenicity (nonviral vectors do not have intrinsic viral coding sequences) (Thomas et al., 2003). Nonviral gene transfer, however, has a comparatively low transfection efficiency, limiting the production of high amounts of the therapeutic protein.

### 3.3.2. Viral vectors

Gene delivery via viral vectors (transduction) is dependent on the natural cellular entry pathways of the viruses they are derived from. Adenoviruses, retroviruses and lentiviruses, herpes simplex virus, baculoviruses, and adeno-associated viruses (AAV) are the most common viruses which have been manipulated so far for gene transfer purposes (Madry et al., 2020b; Robbins et al., 1998).

Adenoviral vectors allow to achieve high transduction efficiencies and elevated transgene expression levels in a variety of cells, enabling direct *in vivo* application, but their use is limited by their immunogenicity and decreased transgene expression over time (1-2 weeks), mostly due to the degradation of the transduced cells by cytotoxic T cells (Cucchiari and Madry, 2010; Rey-Rico and Cucchiari, 2016a). Retroviral vectors may integrate into the genome of the host cells, enabling transgene maintenance over prolonged periods of time, but they have low transduction efficiencies, do not transduce nondividing cells, and carry a risk of insertional mutagenesis that may lead to tumor gene activation (Glass et al., 2014; Murphy et al., 2003; Rey-Rico and Cucchiari, 2016a). Lentiviral vectors display similar properties, although they can transduce both dividing and nondividing cells. Vectors derived from the herpes simplex virus can infect

nondividing cells, yet they are highly toxic and mediate only very short-term transgenic expression (some days) (Rey-Rico and Cucchiaroni, 2016a, 2016b; Robbins and Ghivizzani, 1998; Wu et al., 2013). Baculoviral vectors are not pathogenic and can transduce both dividing and nondividing mammalian cells (Chen et al., 2009) *in vitro* and *in vivo*. However, they do not integrate into the genome of the host cells, resulting in less than one week of transient transgene expression. In marked contrast, due to their unique properties, rAAV vectors are currently the most adapted vehicles for gene transfer *in vitro* and *in vivo*. The basic details will be discussed in the next paragraph. The effectiveness, integration, and features of nonviral and viral vectors are summarized in **Table 1**.

**Table 1.** Gene transfer vectors

Systems	Vectors	Efficacy	Integration	Features
Nonviral	naked plasmid DNA	very low	no	very short-term expression, very low efficiency
	lipoplexes	low	no	short-term expression, low immunogenicity, cytotoxicity at high concentrations
	polyplexes	low	no	short-term expression, low immunogenicity, cytotoxicity at high concentrations
	lipopolyplexes	medium	no	short-term expression, low immunogenicity, low cytotoxicity
	nanoparticles	medium	no	short-term expression, costly, quality control difficulties
	transposons	medium	yes	long-term expression, low immunogenicity, low cytotoxicity
Viral	adenoviral	very high	no	short-term expression, strong immunogenicity
	retroviral	high	yes	long-term expression, strong immunogenicity
	baculoviral	high	no	short-term expression
	rAAV	very high	no	long-term expression, low immunogenicity

Abbreviation: rAAV: recombinant adeno-associated viral vector.

### 3.3.3. rAAV vectors

AAV is a nonpathogenic human parvovirus that is replication-defective. It has been genetically manipulated to form recombinant particles that lack all viral sequences and contain instead a transgene cassette. Hence, this function makes rAAV much less immunogenic compared with adenoviruses vectors that are not completely devoid of viral coding sequences. Although the majority of vectors were initially based on AAV serotype 2 (Samulski et al., 1982), other AAVs (at least 12 naturally occurring serotypes) have been cloned and characterized to date, allowing most types of cells and tissues to be targeted (Grieger and Samulski, 2012; Grimm and Kay, 2003; Wu et al., 2006). rAAV are small vectors (20 nm in diameter) (Cucchiarini and Rey-Rico, 2017) (**Figure 7**) that can transduce both dividing and nondividing cells (Podsakoff et al., 1994; Wu et al., 2006) at very high efficiencies (up to 100%) (Cucchiarini et al., 2011; Madry et al., 2003; Rey-Rico et al., 2015a), enabling direct *in vivo* gene transfer approaches through the dense extracellular matrix (Cucchiarini and Madry, 2014; Cucchiarini et al., 2013; Ulrich-Vinther et al., 2004).

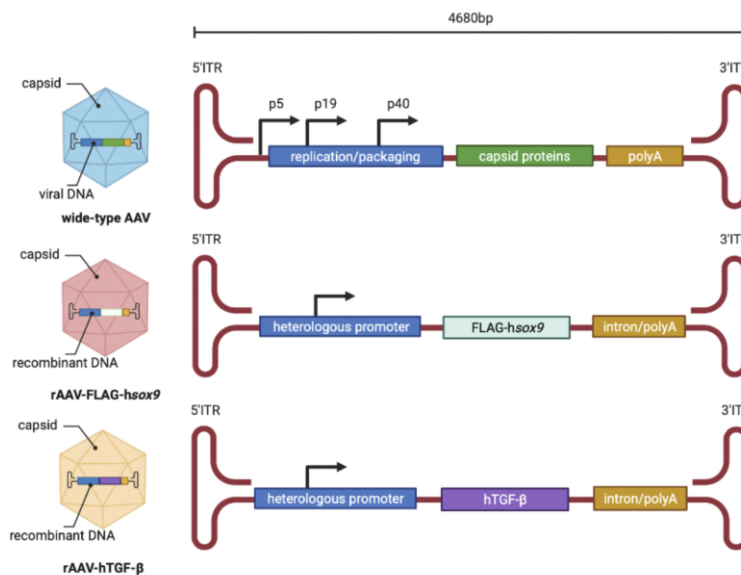


**Figure 7.** Preparation of rAAV gene transfer vectors. The figure shows how rAAV are derived from the wild-type virus with the genes of interest used in the study (SOX9, TGF- $\beta$ ) (created with BioRender.com).

The generation of the trans-splicing vector allowed the vector's size capacity (4.7 kb) to be further increased (Flotte, 2000; Monahan and Samulski, 2000; Sun et al., 2000; Yan et al., 2000). The vector is primarily maintained in transduced cells in stable episomal forms that can be expressed efficiently over prolonged periods of time (from several months to years) (Flotte and Carter, 1995).

### **3.4. Therapeutic candidate: SOX9**

Chondrogenesis is a process highly dependent on the coordination of embryonic development, adult homeostasis, and repair of the vertebrate cartilage (Akiyama and Lefebvre, 2011; Berendsen and Olsen, 2015; Kozhemyakina et al., 2015; Las Heras et al., 2012). Fate decisions and differentiation of chondrocytes involve differential expression of genes essential at each chondrogenic stage.

#### *3.4.1. Functions of SOX9*

SOX9 is a master transcription factor that, by controlling a series of downstream factors (hormones, growth factors, cytokines, transcription factors) in a stage-specific manner, participates in sequential chondrogenic events (Kozhemyakina et al., 2015; Lefebvre and Dvir-Ginzberg, 2017; Symon and Harley, 2017) (**Figure 8**).

SOX9 acts alone or as a trio in conjunction with downstream SOX transcription factors, i.e. SOX5 and SOX6. An attractive system for regenerating damaged cartilage is gene therapy via rAAV in conjunction with biomaterials.

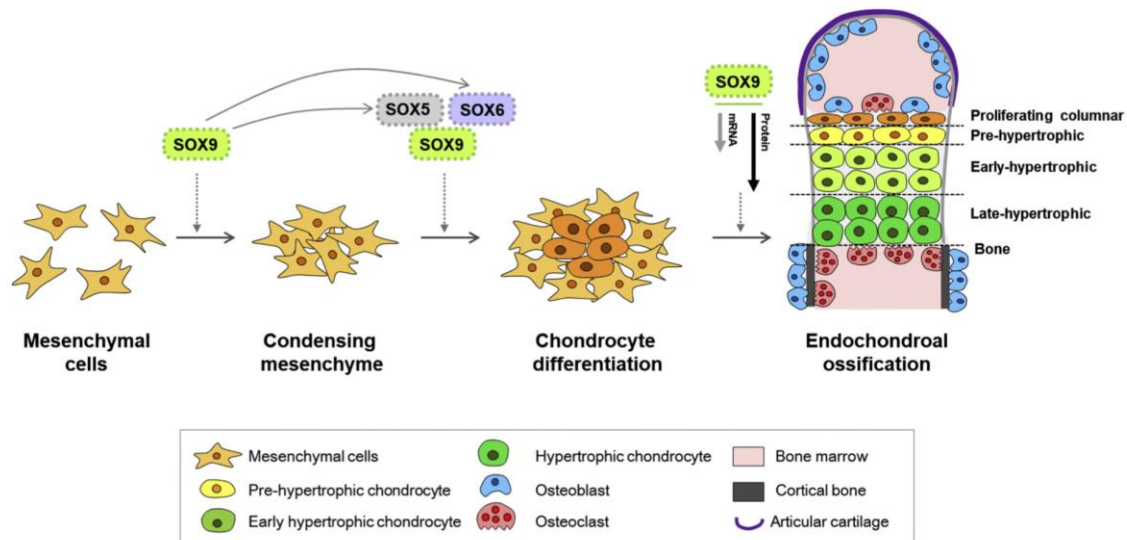


**Figure 8.** Sequential effects of SOX9 on chondrogenesis. Abbreviations: SOX5, sex-determining region Y-type high mobility group box 5; SOX6, sex-determining region Y-type high mobility group box 6; SOX9, sex-determining region Y-type high mobility group box 9. Image from (Song and Park, 2020).

In human individuals, the SOX9 gene is located on chromosome 17, without neighboring protein-coding genes within 3 megabases (Symon and Harley, 2017). The structure of the human SOX9 protein includes 509 amino acids and four functional domains: a high-mobility-group domain, a dimerization domain, and two transactivation domains. SOX9 binds effectively to single or double high-mobility-group-box locations in DNA and thus transactivates its target genes, such as type-II collagen and aggrecan that display stage-specific characteristics for the development of the articular cartilage (Bernard and Harley, 2010; Liu et al., 2017; Symon and Harley, 2017). Whyte *et al.* (Whyte et al., 2013) confirmed that by binding to clusters of enhancers (i.e. super-enhancers) located within and sometimes far upstream of these genes, SOX9 regulates many target genes. Prior work revealed that SOX9 is expressed throughout adulthood in all chondrogenic progenitors and chondrocytes in the articular cartilage, yet its expression abruptly decreases during endochondral ossification in the hypertrophic zone of the growth plate (Zhao et al., 1997). Several studies reported the importance of SOX9 for different stages of chondrogenesis. Among them, Dy *et al.* (Dy et al., 2012) and

Ikegami *et al.* (Ikegami et al., 2011) showed that the half-life of SOX9 protein is longer than that of its mRNA and is therefore present during the early stage of hypertrophy and needed to specifically distinguish hypertrophic chondrocytes until they die or are transformed into osteoblasts. A strong relationship of hypertrophy of chondrocytes between the SOX9 promoter and activator protein-1 family members (such as Jun and Fos12) has been reported in the literature (He et al., 2016). Another study demonstrated that downregulation of SOX9 in the growth plate hypertrophic zone is critical for proper vascular invasion and formation of the bone marrow and, therefore, to successful endochondral ossification (Hattori et al., 2010). Collectively, SOX9 alteration and/or abnormal regulation causes a spectrum of cartilage and/or skeletal development defects and underlies special diseases such as osteoarthritis (OA) (Nishimura et al., 2017) and cancers (Zhang et al., 2017; Zhu et al., 2013). Previous work noted the importance of TGF- $\beta$  to stabilize SOX9 in chondrocytes by activating the canonical small mothers against decapentaplegic (SMAD) and non-canonical p38 pathways (Coricor and Serra, 2016). Gao *et al.* (Gao et al., 2013) indicated that TGF- $\beta$ -activated kinase 1 is primarily a mediator of the bone morphogenetic protein signaling in committed chondrocytes. SOX9 may cooperate with various other SOX family members such as SOX5 and SOX6 that effectively regulate chondrogenic differentiation (Kozhemyakina et al., 2015; Nishimura et al., 2017, 2018). Lefebvre *et al.* (Lefebvre et al., 2001) reported that SOX5, SOX6, and SOX9 play crucial roles in chondrocyte differentiation and, thereby, in cartilage formation. Ikeda *et al.* (Ikeda et al., 2004) found that the SOX trio successfully induced chondrocyte differentiation in all cell types tested, including nonchondrogenic types, and that the induction occurred regardless of the culture system used. The SOX trio suppressed hypertrophic and osteogenic differentiation at the same time (Ikeda et al., 2004). SOX9 expression is affected by various factors and signaling pathways, causing various chondrogenic defects (Kozhemyakina et al., 2015; Li and Dong, 2016; Nishimura et al., 2018). **Tables 2 and 3** present the summary of positive *versus* negative SOX9 regulation, respectively.

**Table 2.** Positive SOX9 regulation

Effectors	Outcomes	References
alginate-encapsulated chondrocytes	increased SOX9 expression/decreased type-I/-X collagen expression in low-density <i>versus</i> monolayer cultures; increased type-II collagen expression in high-density cultures	(Bernstein et al., 2009)
Arid5a	increased chondrocyte-specific activities of SOX9 by direct interaction with Arid5a	(Amano et al., 2011)
CBP/p300	increased SOX9 activities promote cartilage-specific gene expression and chondrocyte differentiation	(Tsuda et al., 2003)
CBP/p300 histone acetylase	increased SOX9 activities promoting COMP expression	(Liu et al., 2007)
exosomal circular RNAs	exosome-transported circular RNA_0001236 enhances chondrogenesis and suppresses cartilage degradation via miR-3677-3P/SOX9 pathway	(Mao et al., 2021)
compressive force	increased chondrogenic nodule formation and type-II collagen, aggrecan, and SOX9 expression; decreased IL-1 $\beta$	(Takahashi et al., 1998)
CREB and Sp1	increased SOX9 proximal promoter region activity	(Piera-Velazquez et al., 2007)
dexamethasone	increased SOX9 and type-II collagen expression	(Sekiya et al., 2001)
ERR- $\alpha$	increased SOX9 expression in C5.18 cells	(Bonnelye et al., 2007)
HC-gp39	increased SOX9 and type-II collagen expression	(Jacques et al., 2007)
HSP60	maintained SOX9 levels by decreased ubiquitination	(Ko et al., 2016)
hypoxia	increased differentiation and proliferation of MSCs via KDM6A expression and SOX9 activation; increased nuclear accumulation of HIF-1 $\alpha$ , activation of the SOX9 promoter, stabilization of the chondrocyte phenotype	(Robins et al., 2005)
IGF-I	increased integrin beta1, Erk, and SOX9 expression; phosphorylated Erk1/2 interacts with SOX9 in chondrocyte nuclei	(Shakibaei et al., 2006)

linc-ROR	linc-ROR modulated MSCs chondrogenesis differentiation and cartilage formation by acting as a competing endogenous RNA for miR-138 and miR-145 and activating SOX9 expression	(Feng et al., 2021)
lncRNA-CRNDE	lncRNA-CRNDE regulates MSC chondrogenic differentiation to promote cartilage repair in OA through SIRT1/SOX9	(Shi et al., 2021)
low levels of SOX9 overexpression	increased type-II collagen expression via specific intronic enhancer in differentiated and slightly phenotypically altered chondrocytes; decreased type-II collagen expression via 263-bp promoter in dedifferentiated chondrocytes	(Kyriotou et al., 2003)
Mg	reduced Mg intake causes cartilage changes that may be secondary to reduced levels of SOX9	(Gruber et al., 2004)
miR-1247	increased chondrocyte-specific activities of SOX9	(Martinez-Sanchez and Murphy, 2013)
PGC-1 $\alpha$	increased SOX9 activities during mouse embryonic limb development and in hMSC chondrogenesis by interaction between PGC-1 $\alpha$ and SOX9	(Kawakami et al., 2005)
PKA-Ca	increased activity of SOX9-dependent type-II collagen chondrocyte-specific enhancers; phosphorylation of SOX9 by PKA increases SOX9 DNA-binding activity to 18-bp and 48-bp type-II collagen enhancer elements	(Huang et al., 2000)
RelA	increased SOX9 expression via binding to an NF- $\kappa$ B binding motif in the SOX9 promoter	(Ushita et al., 2009)
retinoic acid	increased transcriptional activity of the type II-procollagen and SOX9 genes and decreased transcriptional activity of the aggrecan gene promoter/enhancer in TC6 cells with reduced cell proliferation	(Sekiya et al., 2000)
ROCK	increased phosphorylation of SOX9 (Ser181) and activity in SW1353 cells	(Haudenschild et al., 2010)
ROCR lncRNAs	SOX9 induction is ablated in absence of ROCR; SOX9 overexpression rescues MSC differentiation in chondrocytes	(Barter et al., 2017)
SFMBT2	increased SOX9 expression in c28/12 cells	(Hussain et al., 2018)

SOX trio	increased chondrocyte differentiation and decreased hypertrophic and osteogenic differentiation	(Ikeda et al., 2004)
SOX5, SOX6	increased chondrocyte differentiation and cartilage formation	(Lefebvre et al., 2001)
TGFBRI and EGFR	altered expression of TGFBRI and EGFR in diseased chondrocytes; TGF- $\beta$ 3 and EGF modulate the levels of biglycan, SOX9, and RUNX2 in chondrogenic progenitor cells	(Janssen et al., 2019)
ZNF145	increased SOX9 expression	(Liu et al., 2011)

Abbreviations: Arid5a, AT-rich interactive domain-containing protein 5a; CBP/p300, CREB binding protein; RNA, ribonucleic acid; CREB, cyclic adenosine monophosphate response-element binding protein; Sp1, specificity protein 1; ERR- $\alpha$ , estrogen receptor-related receptor alpha; HC-gp39, human cartilage glycoprotein 39; HSP60, heat shock protein 60; IGF-I, insulin-like growth factor I; linc-ROR, long intergenic non-coding RNA, regulator of reprogramming; lncRNA-CRNDE, long non-coding RNA colorectal neoplasia differentially expressed gene; SOX9, sex-determining region Y-type high mobility group box 9; Mg, magnesium; miR, microRNA; PGC-1 $\alpha$ , peroxisome proliferator-activated receptor co-activator 1 alpha; PKA-Ca, cyclic AMP-dependent protein kinase A; RelA, reticuloendotheliosis viral oncogene homolog A (p65 subunit of NF- $\kappa$ B); ROCK, rho kinase; SFMBT2, scm-like with four malignant brain tumor domains 2; SOX trio, SOX5/SOX6/SOX9; TGFBRI, transforming growth factor beta receptor type 1; EGFR, epidermal growth factor receptor; ZNF145, zinc finger protein 145; IL-1 $\beta$ , interleukin 1 beta; COMP, cartilage oligomeric matrix protein; MSCs, mesenchymal stromal cells; KDM6A, Lysine demethylase 6A; HIF-1 $\alpha$ , hypoxia-inducible factor-1 alpha; Erk, extracellular signal-regulated kinase; OA, osteoarthritis; SIRT1, sirtuin 1; bp, base pair; DNA, deoxyribonucleic acid; NF- $\kappa$ B, nuclear factor kappa B; RUNX2, runt-related transcription factor 2.

**Table 3.** Negative SOX9 regulation

Effectors	Outcomes	References
static hyperosmotic conditions	decreased SOX9 expression in OA (but not normal) chondrocytes	(Peffer et al., 2010)
tankyrase	decreased SOX9 expression by PARylation	(Kim et al., 2019)
TGF- $\alpha$	decreased SOX9 expression	(Appleton et al., 2007)
high levels of SOX9 overexpression	decreased type-II collagen expression via a 263-bp short promoter in advanced dedifferentiated chondrocytes and via a 2,266-bp promoter region regardless of the differentiation state of the chondrocytes	(Kypriotou et al., 2003)
ZNF606	decreased SOX9 expression and inhibition of chondrocyte differentiation	(Zhou et al., 2016b)
Twist1	decreased SOX9 activities by binding between SOX9 and Twist1	(Gu et al., 2012)
microRNA-145, microRNA-30a, microRNA-384-5p	decreased SOX9 activities, decreased extracellular matrix formation, including via NF- $\kappa$ B signaling	(Chang et al., 2016; Martinez-Sanchez et al., 2012; Zhang et al., 2018)

Abbreviations: TGF- $\alpha$ , transforming growth factor alpha; RNA, ribonucleic acid; SOX9, sex-determining region Y-type high mobility group box 9; ZNF606, zinc finger protein 606; Twist1, Twist-related protein 1; Twist: transcription factor; microRNA, micro-ribonucleic acid; OA, osteoarthritis; PARylation, poly(ADP-ribosyl)ation; bp, base pair; NF- $\kappa$ B, nuclear factor kappa B.

### 3.4.2. Application of SOX9 to enhance chondrogenesis in vitro

Gene therapy is a unique way of directly transferring therapeutic SOX9 gene sequences to target cells, tissues, and/or organs via a gene carrier. The present paragraph describes relevant, direct (biomaterial-free) SOX9 gene transfer approaches in cells involved in the repair processes of human articular cartilage defects (**Table 4**). Adenoviral gene transfer of SOX9 has been reported early on in hMSCs by Kupcsik et

*al.* (Kupcsik et al., 2010) and next by Weissenberger *et al.* (Weissenberger et al., 2020), allowing to enhance the expression levels of extracellular matrix compounds for 3 weeks. Yet, as this vector class is known for its detrimental and immunogenic effects, a focus was then placed on clinically adapted rAAV gene vehicles to target this cell population. Venkatesan *et al.* (Venkatesan et al., 2012) and Rey-Rico *et al.* (Rey-Rico et al., 2015a) found that following SOX9 gene transfer via rAAV (candidate rAAV-FLAG-hsox9 vector), the expression levels of proteoglycans and type-II collagen increased over time in hMSCs and in human bone marrow aspirates containing concentrated hMSCs with reduced undesirable hypertrophic differentiation *in vitro*. The ability of this rAAV SOX9 therapeutic construct to promote such features makes SOX9 gene transfer via rAAV a best suited strategy for direct translational purposes aiming at enhancing chondrogenic processes in samples from patients.

**Table 4.** Application of SOX9 to enhance chondrogenesis *in vitro*

Treatments	Targets	Outcomes	References
AdV-sox9	hMSCs	increased expression of extracellular matrix compounds (proteoglycans, COMP) for 3 weeks	(Kupcsik et al., 2010)
		increased expression of extracellular matrix compounds (proteoglycans) for 3 weeks	(Weissenberger et al., 2020)
rAAV-FLAG-hsox9	hMSCs	increased expression of extracellular matrix compounds (proteoglycans, type-II collagen) with reduced hypertrophy for 3 weeks	(Venkatesan et al., 2012)
	human bone marrow aspirates	increased expression of extracellular matrix compounds (proteoglycans, type-II collagen) with reduced hypertrophy for 3 weeks	(Rey-Rico et al., 2015a)

Abbreviations: AdV, adenoviral vector; *sox9*, sex-determining region Y-type high mobility group box 9 (cDNA); rAAV, recombinant adeno-associated viral vector; FLAG, tag sequence; hMSCs, human bone marrow-derived mesenchymal stromal cells; COMP, cartilage oligomeric matrix protein.

### 3.4.3. Application of SOX9 to enhance chondrogenesis and cartilage repair *in vivo*

In addition to evaluations *in vitro*, a number of studies examined the potential benefits of SOX9 gene therapy for cartilage repair in relevant experimental (preclinical) animal models *in vivo* (**Table 5**). Adenoviral vector *sox9* gene transfer has been attempted by Cao *et al.* (Cao et al., 2011) to genetically modify MSCs prior to seeding them in a poly(glycolic acid) scaffold and implanting them *in vivo*, promoting enhanced cartilage repair in full-thickness defects for 12 weeks in rabbits. Administration of lentiviral vector *sox9*-modified MSCs seeded in an alginate scaffold within full-thickness defects in rabbits promoted cartilage repair over a period of 12 weeks (Wang et al., 2015). Direct rAAV-FLAG-*hsox9* gene transfer in osteochondral defects was capable of stimulating cartilage repair with delayed hypertrophy in rabbits for at least 16 weeks *in vivo* (Cucchiaroni et al., 2013). These results indicate that SOX9 gene therapy, especially using clinically adapted rAAV vectors, provides promising systems to enhance cartilage repair *in vivo*.

**Table 5.** Application of SOX9 to enhance chondrogenesis and cartilage repair *in vivo*

Treatments	Targets	Outcomes	References
AdV- <i>sox9</i> -modified MSCs seeded in a PGA scaffold	rabbits	increased cartilage repair of full-thickness cartilage defects over a period of 12 weeks	(Cao et al., 2011)
LV- <i>sox9</i> -modified MSCs seeded in an alginate scaffold	rabbits	increased cartilage repair of full-thickness cartilage defects over a period of 12 weeks	(Wang et al., 2015)
rAAV-FLAG- <i>hsox9</i>	rabbits	increased cartilage repair of osteochondral defects over a period of 16 weeks with reduced hypertrophy	(Cucchiaroni et al., 2013)

Abbreviations: AdV, adenoviral vector; *sox9*, sex-determining region Y-type high mobility group box 9 (cDNA); MSCs, marrow-derived mesenchymal stromal cells; PGA, poly(glycolic acid); LV, lentiviral vector; rAAV, recombinant adeno-associated viral vector; FLAG, tag sequence.

### 3.5. Therapeutic gene: TGF- $\beta$

#### 3.5.1. *Functions of TGF- $\beta$*

The family of TGF- $\beta$  contains approximately 35 different pleiotropic polypeptide growth factors (bone morphogenetic proteins, TGF- $\beta$ , activins, growth and differentiation factors) regulating cartilage homeostasis and development (Thielen et al., 2019).

The TGF- $\beta$  signaling is essential for the homeostasis of cartilage and the imbalance results in OA (Blaney Davidson et al., 2009; Chen et al., 2012; Wu et al., 2008). The pathway of SMAD2/3 is activated by the combination between membrane-bound activin-like kinase 5 and TGF- $\beta$  (Remst et al., 2014), while the pathway of SMAD1/5/8 is activated via the combination between membrane-bound activin-like kinase 1 and TGF- $\beta$  (van der Kraan, 2017). The pathway activated type is determined by the TGF- $\beta$  availability (Oliveira Silva et al., 2020) (**Figure 9**).

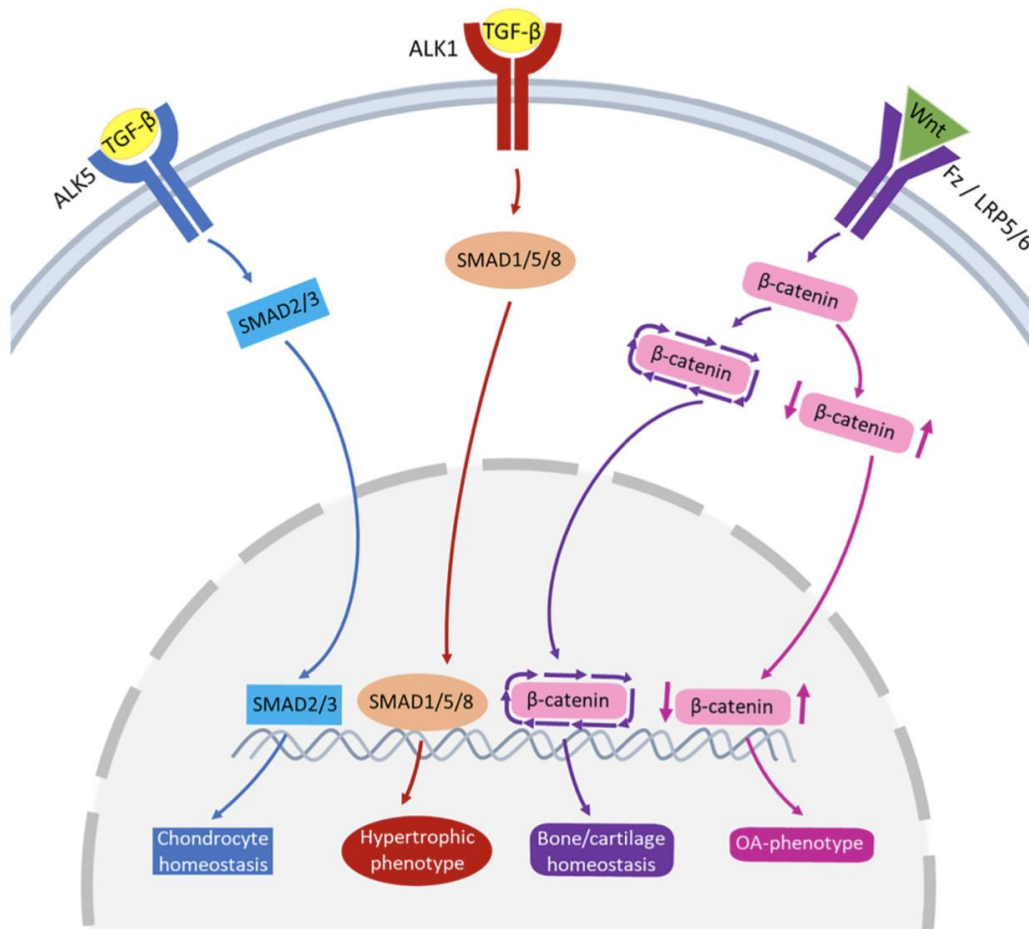


**Figure 9.** Signaling pathways of TGF- $\beta$  and Wnt in joint pathophysiology. TGF- $\beta$  binds to ALK5 to activate SMAD2/3, leading to chondrocyte homeostasis (blue pathway arrows) or to ALK1 to activate SMAD1/5/8, leading to a hypertrophic chondrocyte phenotype (red pathway arrows). Wnt binds to the Fz or LRP5/6 receptors that activate  $\beta$ -catenin synthesis. A healthy expression of  $\beta$ -catenin leads to bone/cartilage homeostasis (purple pathway arrows) while imbalanced  $\beta$ -catenin expression results in an OA phenotype (pink pathway arrows). Abbreviations: ALK, activin-like kinase; TGF- $\beta$ , transforming growth factor beta; Wnt, Wingless and INT-1 (integration); Fz, frizzled; LRP, low density lipoprotein receptor-related protein; SMAD, small mothers against decapentaplegic; OA, osteoarthritis. Image from (Oliveira et al, 2020).

During the normal physiological load in the healthy joints, the signals of TGF- $\beta$  is available readily through the pathway of activin-like kinase 5-SMAD2/3, which drives the protection of cartilage through maintaining the survival and metabolism of chondrocytes (Oliveira Silva et al., 2020). In the pathological environment, for instance, during aging or in OA, the TGF- $\beta$  role may change, and the pathway of activin-like kinase 1-SMAD1/5/8 will be dominant, resulting in the hypertrophic phenotype of chondrocytes, and leading to the imbalance of extracellular matrix conversion (Chen et al., 2012; Li et al., 2010; Retting et al., 2009). The signaling pathways of TGF- $\beta$ /SMAD are crucial for keeping the chondrocytes functions along with the cartilage integrity. The significance of TGF- $\beta$  in OA has been confirmed in many research. The animal models involving genetic changes of TGF- $\beta$  signaling molecules (containing TGF- $\beta$  receptor II overexpression, activin-like kinase 5 knockout and SMAD gene mutation) have the characteristics of OA, containing the chondrocyte differentiation changes and cartilage injury (Blaney Davidson et al., 2006; Serra et al., 1997; Shen et al., 2013; Wang et al., 2017; Yang et al., 2001). SMAD3 gene modified the mice articular cartilage was absent, chondrocyte differentiation was enhanced and proteoglycan was decreased (Yang et al., 2001). The TGF- $\beta$  receptor II specific conditional knockout mice in the chondrocytes developed an OA-like disease characterized by severe cartilage degeneration and chondrocyte hypertrophy (Shen et al., 2013).

TGF- $\beta$  signaling also contributes to cartilage maintenance and integrity by controlling inflammatory cytokine production. The proinflammatory cytokines interleukin 1 beta (IL-1 $\beta$ ) and tumor necrosis factor alpha (TNF- $\alpha$ ) are produced by multiple sources in joint tissues including by the articular chondrocytes (Wojdasiewicz et al., 2014). They are potent inducers of matrix metalloproteinases responsible for cleaving extracellular matrix compounds to maintain normal matrix remodeling and excessive degradation of cartilage during OA (Burrage et al., 2006; Vincenti and Brinckerhoff, 2001; Wojdasiewicz et al., 2014). Matrix metalloproteinase-1 and matrix metalloproteinase-13 are among the most prevalent matrix-degrading enzymes in OA cartilage, targeting type-I, -II, and -III collagen, thus contributing directly to the progression of the disease (Martel-Pelletier et al., 2008; Mitchell et al., 1996; Vincenti et al., 1998). Another key activator of matrix

metalloproteinases in OA tissue is the family of wiggless/integrated glycoproteins. The Wnt signaling pathway has a key role in maintaining cartilage and bone homeostasis (Zhou et al., 2017). TGF- $\beta$  is also critically involved in the stimulation of chondrogenesis (Mackay et al., 1998, 2000) that may affect matrix formation (Verschure et al., 1994). Such effects of TGF- $\beta$  have been further reported via delivery of the factor to MSCs using various hydrogel systems based on chitosan (Kim et al., 2015), gelatin (Lin et al., 2014), hyaluronic acid (Sharma et al., 2007), PEG (Williams et al., 2003), or collagen mimetic peptide (Lee et al., 2006; Makihira et al., 1999), leading to the deposition of cartilaginous extracellular matrix and MSC growth and aggregation.

### 3.5.2. Application of TGF- $\beta$ to enhance chondrogenesis *in vitro*

The present paragraph presents relevant, direct (biomaterial-free) TGF- $\beta$  gene transfer strategies in cells involved in the repair processes of human articular cartilage defects (**Table 6**). Adenoviral vector TGF- $\beta$  gene application was reported by Kawamura *et al.* (Kawamura et al., 2005) and Steinert *et al.* (Steinert et al., 2012) to target hMSCs, increasing the expression of extracellular matrix compounds (proteoglycans, type-II collagen) for up to 3 weeks *in vitro*. Similar results were next obtained with an rAAV-hTGF- $\beta$  candidate vector, improving both extracellular matrix deposition and cell proliferation while favorably reducing hypertrophic differentiation of hMSCs and human bone marrow aspirates over a period of 3 weeks (Frisch et al., 2014, 2016), further confirming the ability of rAAV to deliver therapeutic genes in approaches that aim at stimulating chondrogenic activities in samples from patients.

**Table 6.** Application of TGF- $\beta$  to enhance chondrogenesis *in vitro*

Treatments	Targets	Outcomes	References
AdV-TGF- $\beta$	hMSCs	increased expression of extracellular matrix compounds (proteoglycans, type-II collagen) for 3 weeks	(Kawamura et al., 2005; Steinert et al., 2012)
rAAV-hTGF- $\beta$	hMSCs	increased expression of extracellular matrix compounds (proteoglycans, type-II collagen) and cell proliferation for 3 weeks	(Frisch et al., 2014)
	human bone marrow aspirates	increased expression of extracellular matrix compounds (proteoglycans, type-II collagen) and cell proliferation with reduced hypertrophy for 3 weeks	(Frisch et al., 2016)

Abbreviations: AdV, adenoviral vector; hTGF- $\beta$ , human transforming growth factor beta; rAAV, recombinant adeno-associated viral vector; hMSCs, human bone marrow-derived mesenchymal stromal cells.

### 3.5.3. Application of TGF- $\beta$ to enhance chondrogenesis and cartilage repair *in vivo*

In addition to analyses *in vitro*, various studies evaluated the potential advantages of TGF- $\beta$  gene therapy for cartilage repair in relevant experimental (preclinical) animal models *in vivo* (**Table 7**). Ivkovic *et al.* (Ivkovic et al., 2010) used adenoviral vector TGF- $\beta$  gene transfer to target bone marrow aspirates for implantation in sheep, leading to enhanced cartilage repair in partial-thickness defects for 24 weeks *in vivo*. Application of adenoviral vector TGF- $\beta$ -modified MSCs seeded in demineralized bone matrix in full-thickness defects in pigs enhanced cartilage repair over a period of 12 weeks (Wang et al., 2014). Direct rAAV-hTGF- $\beta$  gene delivery promoted cartilage repair in osteochondral defects in minipigs for 4 16 weeks *in vivo* (Cucchiaroni et al., 2018). These findings demonstrate that TGF- $\beta$  gene therapy, especially via clinically adapted rAAV vectors, is an attractive tool to stimulate cartilage repair *in vivo*.

**Table 7.** Application of TGF- $\beta$  to enhance chondrogenesis and cartilage repair *in vivo*

Treatments	Targets	Outcomes	References
AdV-TGF- $\beta$ -modified bone marrow aspirates	sheep	increased cartilage repair of partial-thickness cartilage defects over a period of 24 weeks	(Ivkovic et al., 2010)
AdV-TGF- $\beta$ -modified MSCs seeded in demineralized bone matrix	pigs	increased cartilage repair of full-thickness cartilage defects over a period of 12 weeks	(Wang et al., 2014)
rAAV-hTGF- $\beta$	minipigs	increased cartilage repair of osteochondral defects over a period of 4 weeks	(Cucchiariini et al., 2018)

Abbreviations: AdV, adenoviral vector; (h)TGF- $\beta$ , (human) transforming growth factor beta; MSCs, mesenchymal stromal cells; rAAV, recombinant adeno-associated viral vector.

### 3.6. Outlook

While successful outcomes were obtained via direct gene therapy using either SOX9 or TGF- $\beta$  in settings that aim at achieving enhanced chondrogenesis and cartilage repair in experimental models *in vitro* and *in vivo*, none gave full satisfaction in terms of complete tissue repair, showing the critical need for improved therapeutic approaches. In this sense, biomaterial-guided gene transfer has a number of advantages over classical gene therapy to tackle chondrogenesis and cartilage repair. In particular, biomaterial-guided gene vector delivery may improve intrinsic cartilage repair mechanisms while protecting against potentially harmful host immune responses that could counteract the gene therapy component. (Cucchiariini and Madry, 2019; Madry et al., 2020b; Rey-Rico and Cucchiariini, 2016a). In this regard, recent work from our Institute revealed the feasibility of delivering SOX9 via rAAV formulated in a thermosensitive poloxamer hydrogel system within sites of cartilage defects in minipigs, promoting chondral repair for 4 weeks *in vivo* (Madry et al., 2020a). While encouraging data were reported, full tissue repair was not achieved in the lesions, supporting the concept of testing novel systems for the controlled release of such vectors in an improved manner.

## 4. HYPOTHESES

The goal of the present work was therefore to evaluate the potential of various carbon dots to associate with and release rAAV vectors as a highly innovative means to target chondrogenically competent hMSCs as a future source of improved reparative cells for cartilage repair, with a focus on transferring DNA sequences for the highly chondroregenerative SOX9 and TGF- $\beta$  factors.

We tested the following two hypotheses:

(1) Carbon dots are potent systems to efficiently vectorize and release rAAV vectors, allowing for an optimal targeting and genetic modification of hMSCs via rAAV gene transfer.

(2) Optimal carbon dots can effectively deliver therapeutic (SOX9, TGF- $\beta$ ) rAAV vectors to reparative hMSCs as a novel, off-the-shelf system for cartilage repair.

## 5. MATERIALS

### 5.1. Chemicals

**Table 8.** Chemicals used in the studies

<b>Products</b>	<b>Manufacturers</b>
AAV titration ELISA	Promega, Heidelberg, Germany
AAVanced concentration reagent	Bioscience, Heidelberg, Germany
ABC reagent (Avidin-biotin-peroxidase reagent)	Alexis Deutschland GmbH, Grünberg, Germany
Acetic acid (1%)	Merck, Darmstadt, Germany
Albumin standard	Thermo Scientific, Rockford, USA
Anti-SOX9 (C-20)	Santa Cruz Biotechnology, Heidelberg, Germany
Anti-TGF- $\beta$ (V)	Santa Cruz Biotechnology, Heidelberg, Germany
Anti-type-I collagen (AF-5610) antibody	Acris, Hiddenhausen, Germany
Anti-type-II collagen (II-II6B3) antibody	Ames, IA, USA
Anti-type-X collagen (COL-10) antibody	Sigma, Taufkirchen, Germany
Atropine	B. Braun, Melsungen, Germany
Beta-Glo <sup>®</sup> assay system kit	Amersham/GE Healthcare, Munich, Germany
Braunol	B. Braun, Melsungen, Germany
BSA (bovine serum albumin)	Sigma, Taufkirchen, Germany
Cell proliferation reagent WST-1	Roche Applied Science, Mannheim, Germany
Cy3 Ab labeling	Roche Applied Science, Mannheim, Germany
DAB (diaminobenzidine) reagent	Vector, Burlingame, California, USA
Eosin G	Roth, Karlsruhe, Germany
Ethanol	Roth, Karlsruhe, Germany
Fast Green	ICN Biomedicals, Eschwege, Germany

Goldner Solution I (Ponceau acid fuchsin)	Roth, Karlsruhe, Germany
Goldner Solution II (Phosphotungstic acid-O)	Roth, Karlsruhe, Germany
Goldner Solution III (light green SF)	Roth, Karlsruhe, Germany
Hamatoxylin	Roth, Karlsruhe, Germany
HCl (1%)	Sigma, Taufkirchen, Germany
Hydrogen peroxide	Sigma, Taufkirchen, Germany
Isoflurane	Baxter, Unterschleißheim, Germany
Ketamine	Ketanest S, Pfizer, Berlin, Germany
Ketavet (Ketamin hydrochlorid)	Pharmacia & Upjohn, Erlangen, Germany
Narcoren (Sodium pentobarbital)	Merial, Hallbergmoos, Germany
Paraffin granules	Roth, Karlsruhe, Germany
Propofol	AstraZeneca, Wedel, Germany
Red blood cell lysing buffer	Sigma, Taufkirchen, Germany
Rompun (Xylazin hydrochloride)	Bayer, Leverkusen, Germany
Roti-Histokitt II (Mounting device)	Roth, Karlsruhe, Germany
Safranin orange	Roth, Karlsruhe, Germany
Sterile saline	B. Braun Medical AG, Melsungen, Germany

## 5.2. Solution and buffers

**Table 9.** Solutions and buffers used in the studies

Solutions, buffers	Ingredients	Weight, volume
Blocking buffer	BSA	6 ml
	PBS	200 ml
DAB solution	H <sub>2</sub> O	5 ml
	Buffer (pH 7.5)	2 drops
	DAB reagent	4 drops
	H <sub>2</sub> O <sub>2</sub>	2 drops

Fast green solution	Fast green	200 mg
	H <sub>2</sub> O	ad 1,000 ml
Eosin solution	Eosin G	10 g
	H <sub>2</sub> O	ad 2,000 ml
	KH <sub>2</sub> PO <sub>4</sub>	9.07 g
	Na <sub>2</sub> HPO <sub>4</sub>	11.86 g
Formalin solution (pH 7.4)	Formalin stock solution	140 ml
	H <sub>2</sub> O	ad 1,000 ml
Haematoxylin solution	Haematoxylin	10 g
	Ethanol (100%)	120 ml
	Sodium iodate	10 g
	ALKSO <sub>4</sub>	200 g
	H <sub>2</sub> O	ad 2,000 ml
HCl solution	HCl (40%)	5.4 ml
	H <sub>2</sub> O	ad 200 ml
PBS	KCL (pH 7.2)	2.7 mM
	K <sub>2</sub> HPO <sub>4</sub>	1.7 mM
	NaCl	136 mM
	Na <sub>2</sub> HPO <sub>4</sub> -7H <sub>2</sub> O	10 mM
Safranin orange solution	Safranin O	1 g
	H <sub>2</sub> O	ad 1,000 ml
Trypsin solution (0.1%)	Trypsin stock solution (25%)	800 µl
	PBS	ad 200 ml
Trypsin stock solution	Trypsin	25% (V/V)
	PBS	75% (V/V)
Hydrogen peroxide (0.3%)	H <sub>2</sub> O <sub>2</sub>	0.6 ml
	H <sub>2</sub> O	200 ml

### 5.3. Equipment

**Table 10.** Equipment used in the studies

<b>Equipment</b>	<b>Manufacturers</b>
Autoclave AMA-240	Astell, Sidcup, England
Canon Powershot A480	Canon, Tokyo, Japan
Digital Camera CC-12 (on Microscope BX-45)	Soft Imaging System, Münster, Germany
Embedding Machine EG 1140-C	Leica, Nussloch, Germany
Refrigerator -20°C	Bosch, Gerlingen-Schillerhöhe, Germany
Refrigerator -74°C Platinum 550	Angelantoni Industrie, Massa Martana PG, Italy
GENios microplate reader	TECAN, Crailsheim, Germany
Incubator CB 150 (37°C)	Binder, Tuttlingen, Germany
Magnetic stirrer RH basic 2	IKA, Staufen, Germany
Microfocus X-ray scanner Skyscan 1172	Skyscan, Kontich, Belgium
Microscopes BX-45 and CK-2	Olympus, Hamburg, Germany
Cover Plate (Plate Sealer)	MD Bioproducts, Saint Paul, USA
Rotational microtome RM 2135	Leica, Nussloch, Germany
Heat plate HI 1220	Leica, Nussloch, Germany
Water bath HI 1210	Leica, Nussloch, Germany

### 5.4. Software

**Table 11.** Software used in the studies

<b>Software</b>	<b>Company</b>
Adobe Photoshop	Adobe Systems, Mountain View, California, USA
AnalySIS	Soft Imaging System GmbH, Münster, Germany
BioRender	BioRender, Toronto, Ontario, Canada

## 6. METHODS

### 6.1. Study design

The goals of the study were to test that: (1) carbon dots are capable of efficiently vectorizing and releasing rAAV vectors, allowing for optimal targeting and genetic modification of hMSCs through rAAV gene transfer, and (2) optimal carbon dots can deliver therapeutic (SOX9, TGF- $\beta$ ) rAAV vectors to reparative hMSCs as a novel, off-the-shelf system for cartilage repair.

### 6.2. Preparation of hMSCs

The study was approved by the Ethics Committee of the Physicians Saarland Council (*Ärztammer des Saarlandes*, reference number Ha06/08). Prior to including patients in the evaluations, they were asked for their informed consent under the Helsinki Declaration. Upon consent, patients undergoing a total knee arthroplasty (age between 75 and 3 years, with patient number of 12) were selected and bone marrow aspirates were collected from the distal femurs ( $0.4\text{-}1.2 \times 10^9$  cells/ml, approximately 15 ml). Using Dulbecco's modified Eagle's Medium (DMEM), bone marrow-derived hMSCs were separated via centrifugation followed by washing and resuspension in DMEM using red blood cell lysing buffer/DMEM (1:1) (Frisch et al., 2014; Venkatesan et al., 2012). The mixtures were washed and resuspended in fetal bovine serum (10%), streptomycin (100  $\mu\text{l/ml}$ ), and penicillin (100 U/ml) (growth medium) for cell maintenance and plating in T-75 flasks under 5% CO<sub>2</sub> at 37°C. Growth medium containing 1 ng/ml recombinant FGF-2 (Frisch et al., 2014; Venkatesan et al., 2012) was applied to replace the medium after one day, and the medium was then replaced every two to three days. The cells were replated when the cell density reached 85% and used at passage 1-2.

### 6.3. Preparation of carbon dots

Four carbon dots (CD-1 to CD-4) were created using a bottom-up method where citric acid was exploited as the carbon source with the aid of a variety of additives as passivators: branched poly(ethyleneimine) 600 Da, *N,N*-dimethylethylenediamine, and pentaethylenehexamine, PEG monomethyl ether 550 Da or PEG monomethyl ether 2000 Da (Fan et al., 2019; Pierrat et al., 2015) (**Figure 10** and **Table 11**). After pyrolysis under irradiation with microwave or conventional heating, the systems were extensively dialysed and purified with 0.1 N HCl and 1,000 Da ultra-pure H<sub>2</sub>O (Fan et al., 2019; Pierrat et al., 2015). The carbon dots were freeze-dried and 5.0 mg/ml stock solutions were prepared and stored at 4°C until use (Fan et al., 2019; Pierrat et al., 2015). For the nanoparticles, the charge and size (zeta potential,  $\zeta$ ) were detected with dynamic light scattering and transmission electron microscopy ((NanoSizer NanoZS, Malvern UK) using a voltage of 5 kV (LVEM5, Delong Instruments, Brno, Czech Republic) (Fan et al., 2019; Pierrat et al., 2015) (**Table 11**).

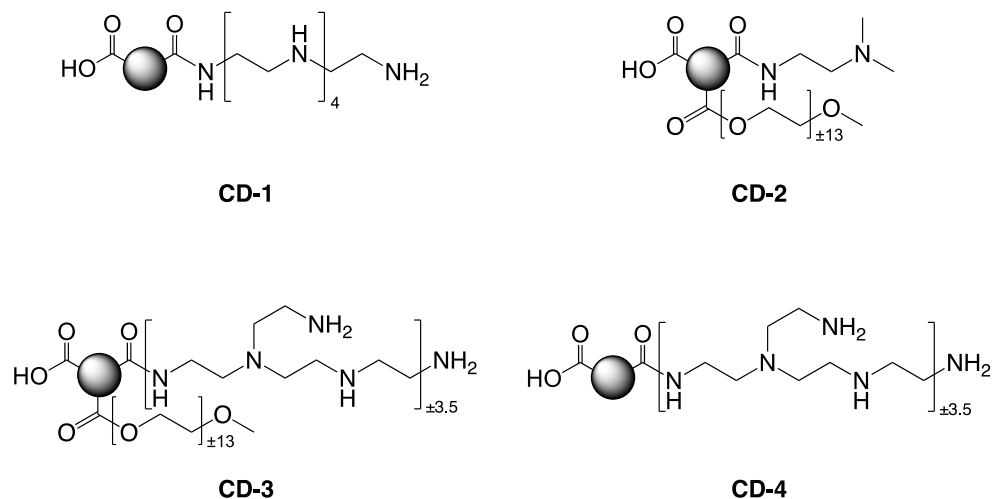


**Figure 10.** Structural features of the various carbon dots tested in the studies. The carbon dots CD-1 to CD-4 were generated through pyrolysis of citric acid in the presence of various passivation reagents presented in the Materials and Methods and in **Table 11**. Abbreviation: CD, carbon dot. Image from (Meng et al., 2020).

**Table 12.** Characteristics of the carbon dots (CD-1 to CD-4) employed in the studies

Name	Starting material (w/w)	Activation mode	Size (nm) <sup>a</sup>		$\zeta$ potential <sup>a</sup> (mV)
			DLS	TEM	
CD-1	CA/PEHA (1/4)	1) 30 min at 180°C <sup>b</sup> 2) 30 min at 230°C <sup>b</sup>	36.4 ± 12.0	17.9	+18.6 ± 0.9
CD-2	CA/mPEG <sub>550</sub> /DMEDA (1/3/3)	1) 30 min at 180°C <sup>b</sup> 2) 30 min at 230°C <sup>b</sup>	17.7 ± 0.9	16.3	+26.9 ± 1.6
CD-3	CA/bPEI <sub>600</sub> /mPEG <sub>2000</sub> (1/4/1)	microwave 620 W, 190 sec <sup>c</sup>	13.3 ± 0.4	-	+29.4 ± 0.4
CD-4	CA/bPEI <sub>600</sub> (1/4)	microwave 620 W, 120 sec <sup>c</sup>	11.7 ± 0.9	-	+37.6 ± 3.2

<sup>a</sup>Measured at 1.0 mg/ml in 1.5 mM NaCl, pH 7.4. <sup>b</sup>Reactions were conducted under conventional heating. <sup>c</sup>Reactions were conducted in a domestic microwave oven. Abbreviations: bPEI<sub>600</sub>, branched poly(ethyleneimine) 600 Da; CA, citric acid; CD, carbon dot; DLS, dynamical light scattering; DMEDA, *N,N*-dimethylethylenediamine; mPEG<sub>550</sub>, poly(ethylene glycol) monomethyl ether 550 Da; mPEG<sub>2000</sub>, poly(ethylene glycol) monomethyl ether 2000 Da; PEHA, pentaethylenhexamine; TEM, transmission electron microscopy.

#### 6.4. Preparation of rAAV vectors

The vectors were generated using pSSV9, a parental AAV serotype 2 genomic clone (Samulski et al., 1987, 1989). rAAV-*lacZ* carries the *E. coli*  $\beta$ -galactosidase ( $\beta$ -gal) reporter gene (*lacZ*), rAAV-FLAG-hsox9 a 1.7-kb FLAG-tagged human *sox9* (*hsox9*) cDNA sequence, and rAAV-hTGF- $\beta$  a 1.2-kb human TGF- $\beta$ 1 (hTGF- $\beta$ ) sequence, all controlled by the cytomegalovirus immediate-early promoter (Frisch et al., 2014; Rey-Rico et al., 2016; Venkatesan et al., 2012). Conventional packaging of not self-

complementary vectors was performed using helper-free (two-plasmid) transfection in 293 cells with the packaging plasmid pXX2 and the adenoviral helper plasmid pXX6 (Frisch et al., 2014; Rey-Rico et al., 2016). Vector purification was performed using the AAVanced Concentration Reagent (Rey-Rico et al., 2016) and vector titers were monitored by real-time PCR (Frisch et al., 2014; Rey-Rico et al., 2016; Venkatesan et al., 2012), averaging  $10^{10}$  transgene copies/ml (~1/500 functional recombinant viral particles).

### **6.5. Cy3 labeling**

In accordance with the recommendations of the manufacturer, rAAV vectors were labeled using the Cy3 Ab Labeling kit by mixing 1 ml of rAAV in a buffer composed of sodium bicarbonate and sodium carbonate at pH 9.3 at room temperature for half an hour, then labeled using Cy3 and dialyzed with NaCl (150 ml)/HEPES (20 mm) at pH 7.5 (Rey-Rico et al., 2016).

### **6.6. Complexation of rAAV vectors with carbon dots and release studies**

40  $\mu$ l of rAAV vectors (transgene copies:  $8 \times 10^5$ ) were mixed with a variety of carbon dots (40  $\mu$ l) directly and cultured at environmental temperature for half an hour to create the systems of rAAV/carbon dot. In addition, the visual analysis for complexation researches was performed by mixing 40  $\mu$ l carbon dots with 40  $\mu$ l of rAAV labeled with Cy3 (transgene copies:  $8 \times 10^5$ ) on a 100  $\mu$ l serum-free DMEM on the 96-well plates using a rAAV vector labeled with Cy3. The monitoring of samples with Cy3 labeling were conducted using the rhodamine filter under real-time fluorescence (Olympus CKX41, Hamburg, Germany). The rAAV/carbon dot systems generated were maintained in 24-well plates and serum-free DMEM (350  $\mu$ l), and the presence of rAAV in the medium was determined by AAV titration ELISA at the specified time points (Rey-Rico et al., 2016).

## 6.7. rAAV/carbon dot-mediated gene transfer

Monolayer cultures of hMSCs were directly incubated with the rAAV/carbon dot systems prepared as described above in the various assays at the indicated cell densities, culture formats, and volume/multiplicity of infection (MOI) (Frisch et al., 2014; Rey-Rico et al., 2016; Venkatesan et al., 2012). The cultures were kept in humidified air containing 5% CO<sub>2</sub> in growth medium (Frisch et al., 2014; Venkatesan et al., 2012) for 21 days at 37°C to carry out the various analyses.

## 6.8. Analysis of transgene expression

The expression of *lacZ* was monitored under light microscopy (Olympus BX45) using X-Gal staining and also employing the Beta-Glo<sup>®</sup> Assay System to assess the β-gal activities as Relative Luminescence Units with standardization to the cell numbers (Rey-Rico et al., 2016). Expression of TGF-β and SOX9 was detected by immunohistochemistry via application of specific primary antibodies, biotinylated secondary antibodies, and the ABC approach and utilizing diaminobenzidine as the chromogen for examination under light microscopy (Olympus BX45) (Frisch et al., 2014; Venkatesan et al., 2012). A specific ELISA was employed to determine the concentrations of TGF-β (Frisch et al., 2014). All quantitative measurements were performed on a GENios fluorometer/spectrophotometer (Tecan, Crailsheim, Germany).

## 6.9. Cell viability and proliferation

The Cell Proliferation Reagent WST-1 was utilized to monitor the viability of the cells based on the analysis of OD<sup>450 nm</sup> that is proportional to the cell numbers applied (Frisch et al., 2014; Rey-Rico et al., 2016; Venkatesan et al., 2012). The proliferation of cell was regarded as the direct indicator (Frisch et al., 2014; Venkatesan et al., 2012). The calculation for the percentage of cell viability (Rey-Rico et al., 2016) was carried out as:

$$\text{cell viability (\%)} = [\text{absorbance of the sample/absorbance of the negative control}] \times 100$$

All measurements were performed using a GENios spectrophotometer/fluorometer (Tecan).

## **6.10. Histology and immunohistochemistry**

At the specified time points, the monolayer cultured cells were collected and fixed with 4% of formalin. As reported earlier (Rey-Rico et al., 2016), alcian blue was applied to stain the fixed cells for an analysis of glycosaminoglycans and the excess staining was removed in double distilled water. Using a GENios fluorometer/spectrophotometer, specific OD<sup>600 nm</sup> was measured via dissolution in guanidine hydrochloride (6 M) (Rey-Rico et al., 2016) and alcian blue staining was estimated quantitatively. Immunohistochemical assessments of type-I, -II, and -X collagen deposition were carried out using a light microscope (Olympus BX45) based on specific primary antibodies, biotinylated secondary antibodies, as well as the ABC approach and DAB (Frisch et al., 2014; Rey-Rico et al., 2016; Venkatesan et al., 2012). Control conditions lacking the primary antibody were also performed for the detection of the secondary immunoglobulins.

## **6.11. Histomorphometric analyses**

The extent of X-Gal staining and the percentage of cells positively expressing TGF- $\beta$ , SOX9, and type-I/-II/-X collagens to the total number of cells were evaluated on three random positions in the cultures or sections employing the Adobe Photoshop (Adobe Systems, Unterschleissheim, Germany) and an analysis SIS software (Olympus) (Frisch et al., 2014; Rey-Rico et al., 2016).

## **6.12. Statistical analysis**

Data are provided as mean  $\pm$  standard deviation (SD) of separate experiments. Each condition was performed in triplicate in three independent experiments per patient. Data were obtained by two individuals blinded with respect to the groups. The t-test and the Mann-Whitney Rank Sum test were used where appropriate. A *P* value of less than 0.05 was considered statistically significant.

## 7. RESULTS

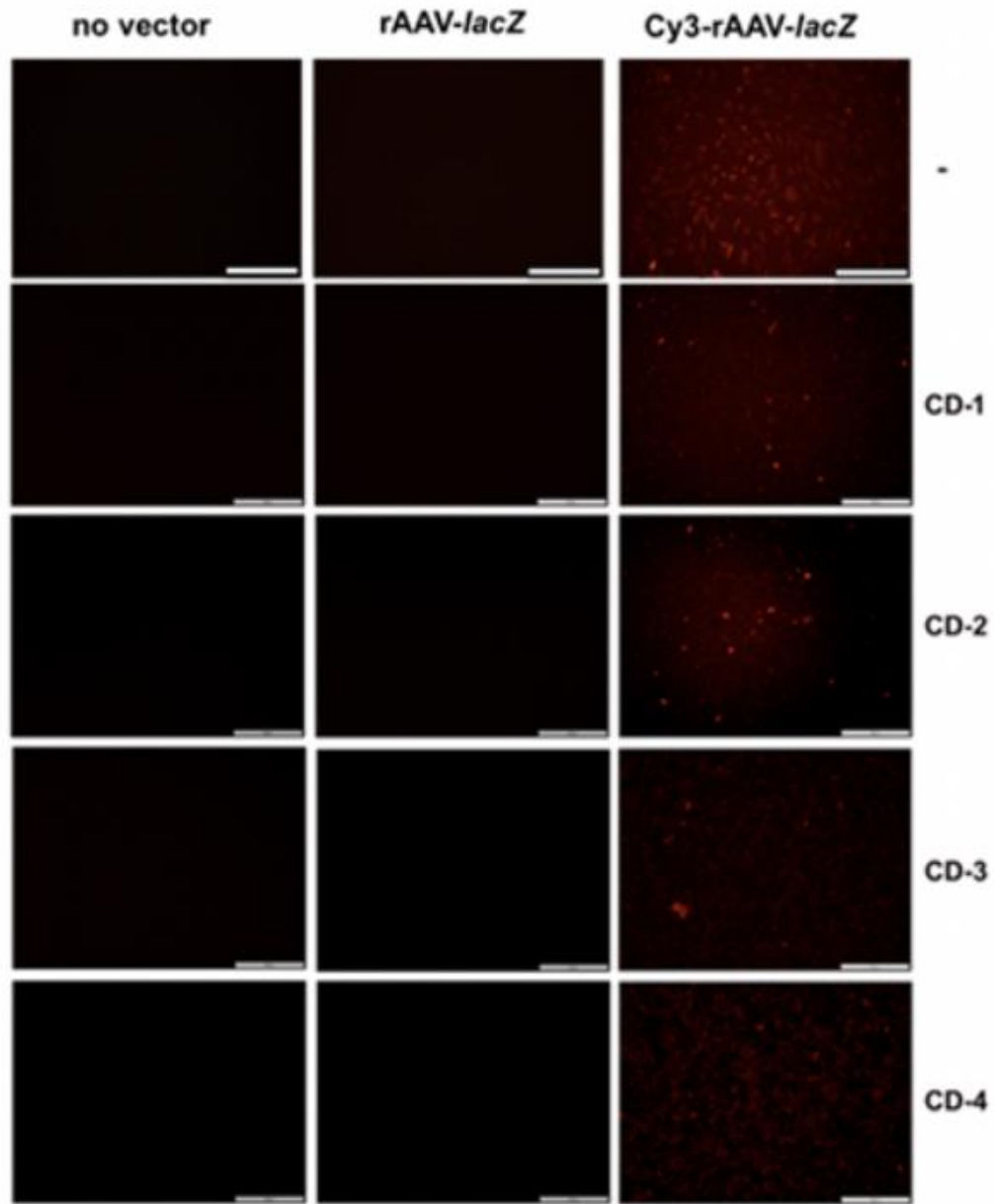
### 7.1. Effective rAAV association to carbon dots and release

The reporter rAAV-*lacZ* vector was first formulated with the various carbon dots (CD-1 to CD-4) to measure the ability of the systems to engineer and release rAAV over a 10-day period, the longest time period tested. In parallel, rAAV-*lacZ* was labeled with Cy3 to enable visualization of the vector in the carbon dot systems.

Active Cy3 fluorescence in the Cy3-labeled-rAAV-*lacZ*/carbon dot samples was effectively detected after twenty-four hours compared with various control conditions (carbon dots without rAAV-*lacZ*, carbon dots with unlabeled rAAV-*lacZ*) (**Figure 11A**), indicating that rAAV vectors were successfully formulated in the various carbon dots, without difference between the various carbon dots.

An estimation of the rAAV capsid concentrations in culture medium showed that all the carbon dots were capable of releasing rAAV over a 10-day span (**Figure 11B**), with CD-2 allowing for the earliest vector release and good vector concentration maintenance over time (rAAV-*lacZ*/CD-2) with the other carbon dots (rAAV-*lacZ*/CD-1, rAAV-*lacZ*/CD-3, and rAAV-*lacZ*/CD-4) and with free vector control (rAAV-*lacZ*).

**A.**



**B.**

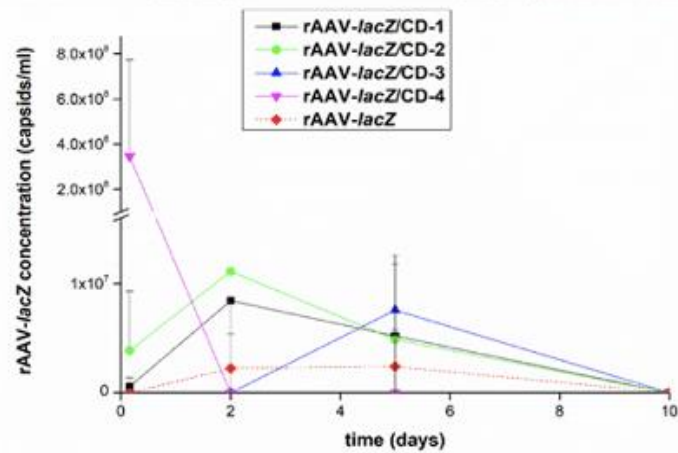


**Figure 11.** Complexation and release of rAAV from the carbon dots. rAAV-*lacZ* was labeled with Cy3 and formulated with the carbon dots (40  $\mu$ l rAAV,  $8 \times 10^5$  transgene copies/40  $\mu$ l carbon dots) and placed in culture over time. **(A)** Cy3-labeled rAAV in the carbon dots were observed under live fluorescence after 24 h (magnification x10; scale bars: 100  $\mu$ m; representative data). Control conditions included carbon dot formulations with unlabeled rAAV, carbon dots lacking rAAV, and the absence of carbon dots. **(B)** rAAV release from the carbon dots was monitored by measuring rAAV concentrations in the culture medium at the denoted time points using an AAV titration ELISA. Free vector treatment was used as a control condition. Abbreviations: rAAV, recombinant adeno-associated viral vector; CD, carbon dot. Image from (Meng et al., 2020).

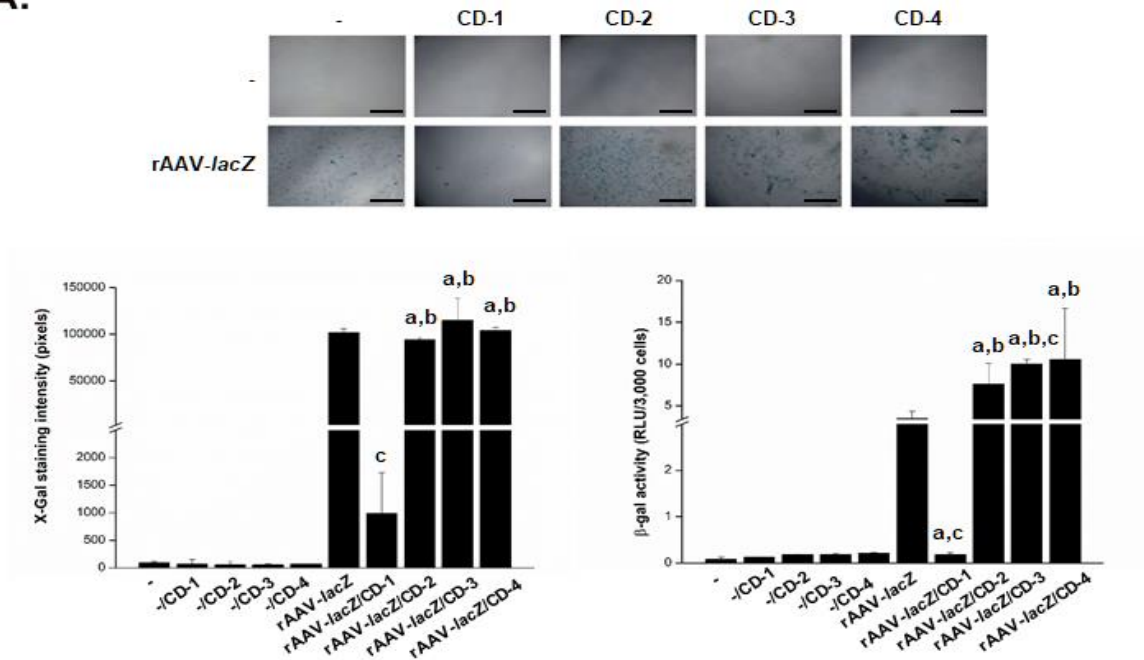
## 7.2. Effective carbon dot-guided, rAAV-mediated reporter *lacZ* overexpression in hMSCs

The reporter rAAV-*lacZ* vector was then formulated with the various carbon dots (CD-1 to CD-4) to test the systems' ability to facilitate the genetic modification of hMSCs over 10 days, the longest time point tested, compared with control conditions (carbon dots missing rAAV, i.e. -/CD; free rAAV, i.e. rAAV-*lacZ*; absence of both carbon dots and rAAV, i.e.-).

The estimated extent of X-Gal staining in cells on day one indicated that the CD-4, CD-2, and CD-3 preparations of rAAV-*lacZ* could promote *lacZ* expression in hMSCs, with no apparent difference compared with free vector administration ( $P \geq 0.050$ ) (**Figure 12A**). After 10 days, the staining intensities in cells treated with rAAV-*lacZ*/CD-4, rAAV-*lacZ*/CD-3, and rAAV-*lacZ*/CD-2 increased, particularly when treated via CD-2 (1.4-fold increase *versus* day 1;  $P = 0.060$ ), and there was no difference compared with treatment with free rAAV-*lacZ* ( $P \geq 0.050$ ) (**Figure 12B**). In contrast to free vector administration, rAAV-*lacZ* distribution via CD-1 greatly reduced such staining intensities in hMSCs (102.9- and 32.5-fold decrease on days 1 and 10, respectively; always  $P \leq 0.040$ ) (**Figures 12A and 12B**). An assessment of the  $\beta$ -gal activities in the cells using the Beta-Glo<sup>®</sup> Assay confirmed these results, with even higher activities when rAAV-*lacZ*

was delivered via CD-2, CD-3, or CD-4 *versus* free vector treatment (up to 2.9- and 2.3-fold difference on days 1 and 10, respectively; always  $P \leq 0.050$ ), and lower activities when CD-1 was employed (19- and 15.8-fold difference *versus* free vector administration; always  $P \leq 0.020$ ) (**Figures 12A and 12B**).

**A.**



**B.**

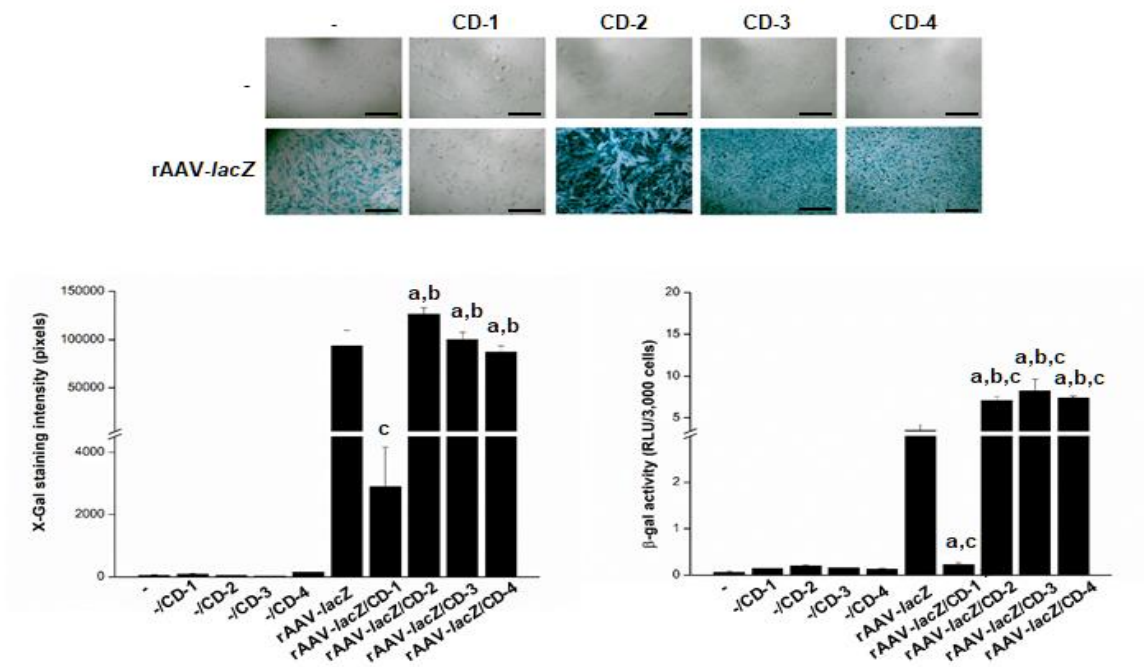


**Figure 12.** Detection of reporter (*lacZ*) overexpression in hMSCs transduced with the rAAV/carbon dot systems. rAAV-*lacZ* (20  $\mu$ l,  $4 \times 10^5$  transgene copies) was formulated with the carbon dots (CD-1 to CD-4; 20  $\mu$ l) and the rAAV/carbon dot systems (40  $\mu$ l, i.e.  $4 \times 10^5$  transgene copies) were incubated with hMSCs (3,000 cells in 96-well plates; MOI = 133) for up to 10 days. Expression of *lacZ* was tested by X-Gal staining (top panel: magnification x4; scale bars: 500  $\mu$ m; representative data) with corresponding histomorphometric analyses (bottom left panel) and by quantitative estimation of the  $\beta$ -gal activities using the Beta-Glo<sup>®</sup> Assay System (bottom right panel) after one (**A**) and 10 days (**B**). Control conditions included carbon dots lacking rAAV (-/CD), free rAAV (rAAV-*lacZ*), and absence of both carbon dots and rAAV (-). Statistically significant relative to <sup>a</sup>-, <sup>b</sup>-/CD, and <sup>c</sup>rAAV-*lacZ*. Abbreviations: CD, carbon dot; recombinant adeno-associated viral vector; hMSCs, human bone marrow-derived mesenchymal stromal cells. Image from (Meng et al., 2020).

According to the results of a WST-1 assay, carbon dot-guided delivery of rAAV-*lacZ* to hMSCs using either CD-1 or CD-2 was safe, with 100% cell viability maintained on day 1 and no significant difference compared with the corresponding control conditions (-, -/CD-1, -/CD-2, and free vector administration; always  $P \geq 0.180$ ) (**Figure 13A**). In contrast, CD-3 and CD-4 had significantly detrimental effects on cell viability (< 32%; always  $P \leq 0.010$  versus all other conditions). On day 10, similar observations were recorded, with 100% viability using CD-1 and CD-2 as in the control conditions (always  $P \geq 0.050$ ) and about 25-30% viability using CD-3 or CD-4 (always  $P \leq 0.040$  versus all other conditions) (**Figure 13B**).

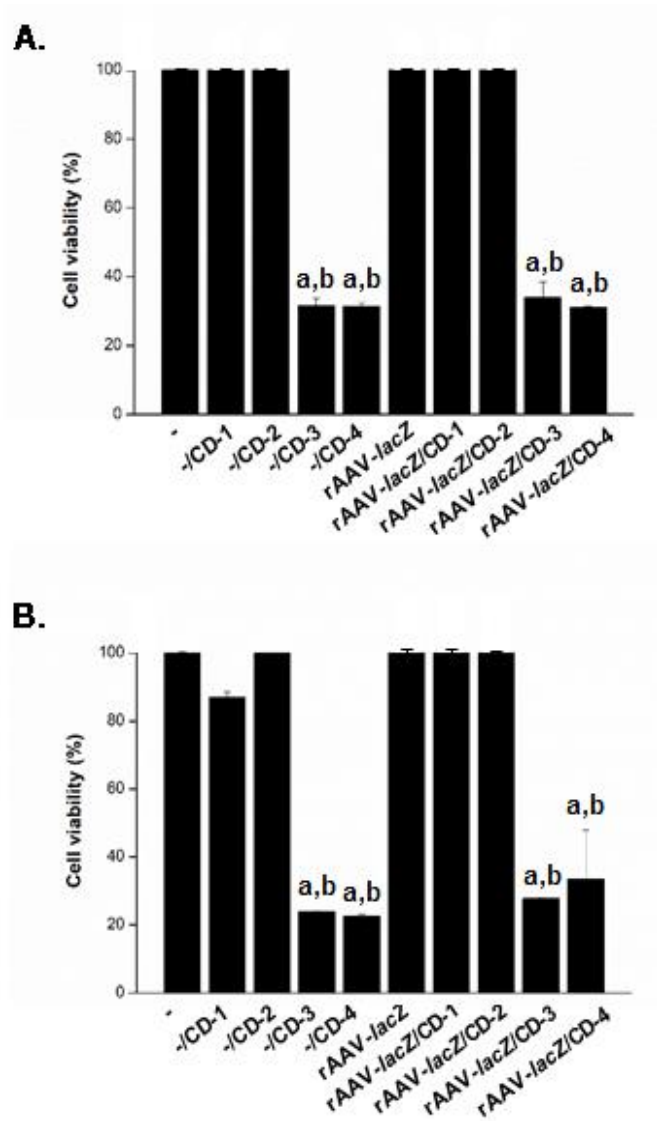


**Figure 13.** Cell viability in hMSCs transduced with the rAAV/carbon dot systems. rAAV-*lacZ* (20  $\mu$ l,  $4 \times 10^5$  transgene copies) was formulated with the carbon dots (CD-1 to CD-4; 20  $\mu$ l) and the rAAV/carbon dot systems (40  $\mu$ l, i.e.  $4 \times 10^5$  transgene copies) were incubated with hMSCs (3,000 cells in 96-well plates; MOI = 133) for up to 10 days. Cell viability was examined after one (**A**) and 10 days (**B**) using the Cell Proliferation Reagent WST-1. Control conditions included carbon dots lacking rAAV (-/CD), free rAAV (rAAV-*lacZ*), and absence of both carbon dots and rAAV (-). Statistically significant relative to <sup>a</sup>- and <sup>b</sup>rAAV-*lacZ*. Abbreviations: CD, carbon dot; rAAV, recombinant adeno-associated viral vector. Image from (Meng et al., 2020).

### 7.3. Effective carbon dot-guided, rAAV-mediated SOX9 and TGF- $\beta$ overexpression in hMSCs

In light of the efficacy and safety of CD-2, the therapeutic rAAV-FLAG-hsox9 and rAAV-hTGF- $\beta$  were next formulated independently with this system (rAAV-FLAG-hsox9/CD-2 and rAAV-hTGF- $\beta$ /CD-2, respectively) to determine the ability of CD-2 to promote the overexpression of each candidate gene (SOX9, TGF- $\beta$ ) via rAAV in hMSCs over 21 days, the longest time point evaluated, relative to control conditions (CD-2 lacking rAAV, i.e. -/CD-2; CD-2 formulating rAAV-*lacZ*, i.e. rAAV-*lacZ*/CD-2).

After 21 days, an immunocytochemical analysis of SOX9 expression showed that rAAV-FLAG-hsox9 administered to hMSCs via CD-2 resulted in significantly higher levels of SOX9 expression than all other conditions (65-, 43.3-, and 1.8-fold difference using rAAV-FLAG-hsox9/CD-2 *versus* -/CD-2, rAAV-*lacZ*/CD-2, and rAAV-hTGF- $\beta$ /CD-2, respectively; always  $P \leq 0.001$ ) (**Figure 14A** and **Table 12**).

An evaluation of TGF- $\beta$  expression by immunocytochemistry also showed that delivery of rAAV-hTGF- $\beta$  to hMSCs via CD-2 led to significantly higher levels of TGF- $\beta$  expression relative to all other conditions after 21 days (10.3-, 6.8-, and 9.4-fold difference using rAAV-hTGF- $\beta$ /CD-2 *versus* -/CD-2, rAAV-*lacZ*/CD-2, and rAAV-FLAG-hsox9/CD-2, respectively; always  $P \leq 0.001$ ) (**Figure 14B** and **Table 12**). This result was corroborated by an estimation of the levels of TGF- $\beta$  production in the cells by ELISA, with up to 2.8-, 2.8-, and 3.8-fold higher TGF- $\beta$  secretion levels when using rAAV-hTGF- $\beta$ /CD-2 after 5, 7, and 21 days, respectively, *versus* all other conditions (always  $P \leq 0.001$ ) (**Figure 14B**).

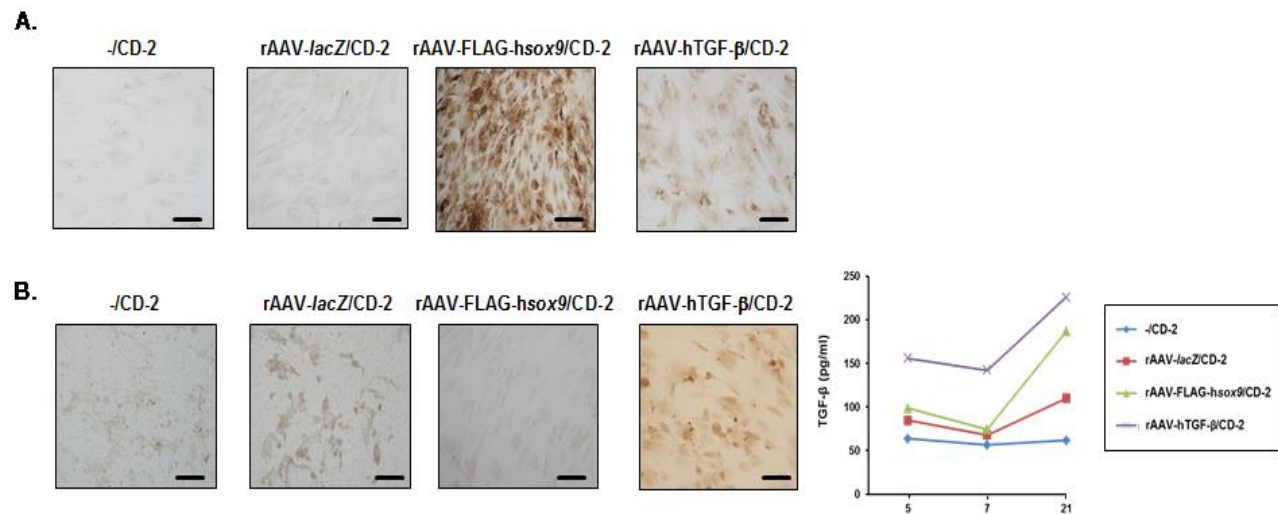


**Figure 14.** Detection of therapeutic (SOX9, TGF- $\beta$ ) gene overexpression in hMSCs transduced with rAAV/CD-2. The rAAV-FLAG-*hsox9*, rAAV-hTGF- $\beta$ , and rAAV-*lacZ* vectors (40  $\mu$ l each vector,  $8 \times 10^5$  transgene copies) were formulated with CD-2 (40  $\mu$ l) and the rAAV/CD systems (80  $\mu$ l, i.e.  $8 \times 10^5$  transgene copies) were incubated with hMSCs (10,000 cells in 48-well plates; MOI = 80) for up to 21 days. SOX9 (**A**) and TGF- $\beta$  (**B**) expression was examined by immunocytochemistry (**A**, **B**; magnification x20; scale bars: 50  $\mu$ m; representative data) and by specific (TGF- $\beta$ ) ELISA (**B**). rAAV-*lacZ*/CD-2 and CD-2 lacking rAAV were used as controls. Abbreviations: CD, carbon dot; rAAV, recombinant adeno-associated viral vector; *sox9*, sex-determining region Y-type high mobility group box 9 (cDNA); SOX9, protein; TGF- $\beta$ , transforming growth factor beta (cDNA or protein). Image from (Meng et al., 2020).

**Table 13.** Histomorphometric analyses in hMSCs transduced with rAAV/CD-2

Parameter	-/ CD-2	rAAV- <i>lacZ</i> / CD-2	rAAV-FLAG- <i>hsox9</i> / CD-2	rAAV-hTGF- $\beta$ / CD-2
SOX9	1.5 $\pm$ 0.6	2.3 $\pm$ 0.5	97.5 $\pm$ 1.3 <sup>a,b</sup>	52.8 $\pm$ 2.2 <sup>a,b,c</sup>
TGF- $\beta$	7.8 $\pm$ 3.1	11.8 $\pm$ 2.4	8.5 $\pm$ 1.3	79.8 $\pm$ 3.9 <sup>a,b,c</sup>
Type-II collagen	4.8 $\pm$ 2.5	5.5 $\pm$ 2.6	84.8 $\pm$ 2.2 <sup>a,b</sup>	68.5 $\pm$ 4.5 <sup>a,b,c</sup>
Type-I collagen	85.3 $\pm$ 2.2	85.8 $\pm$ 2.6	4.3 $\pm$ 1.7 <sup>a,b</sup>	3.8 $\pm$ 1.0 <sup>a,b</sup>
Type-X collagen	73.3 $\pm$ 1.7	72.3 $\pm$ 1.7	11.8 $\pm$ 1.7 <sup>a,b</sup>	12.8 $\pm$ 1.7 <sup>a,b</sup>

Values are given as mean  $\pm$  SD. All parameters are in % of positively (SOX9<sup>+</sup>, TGF- $\beta$ <sup>+</sup>, type-II<sup>+</sup>/I<sup>+</sup>/X<sup>+</sup> collagen) stained cells to the total cell numbers. Statistically significant relative to <sup>a</sup>-/CD-2, <sup>b</sup>rAAV-*lacZ*/CD-2, and <sup>c</sup>rAAV-FLAG-*hsox9*. Abbreviations: CD, carbon dot; rAAV, recombinant adeno-associated viral vector; *sox9*, sex-determining region Y-type high mobility group box 9 (cDNA); SOX9, protein; TGF- $\beta$ , transforming growth factor beta (cDNA or protein). Image from (Meng et al., 2020).

#### 7.4. Effects of carbon dot-guided, rAAV-mediated SOX9 and TGF-beta overexpression on the biological activities in hMSCs

With the formulations rAAV-FLAG-*hsox9*/CD-2 and rAAV-hTGF- $\beta$ /CD-2, the ability of CD-2 to trigger biological activities (cell proliferation, matrix deposition) in hMSCs over time (21 days) was compared with control conditions (-/CD-2, rAAV-*lacZ*/CD-2).

Administration of rAAV-hTGF- $\beta$  in hMSCs via CD-2 led to significantly higher levels of cell proliferation relative to all other conditions after 21 days (1.3-, 1.3-, and 1.2-

fold difference using rAAV-hTGF- $\beta$ /CD-2 *versus* -/CD-2, rAAV-*lacZ*/CD-2, and rAAV-FLAG-hsox9/CD-2, respectively; always  $P \leq 0.001$ ), while no difference was seen with rAAV-FLAG-hsox9/CD-2 ( $P \geq 0.065$  *versus* -/CD-2 or rAAV-*lacZ*/CD-2) (**Figure 15A**).

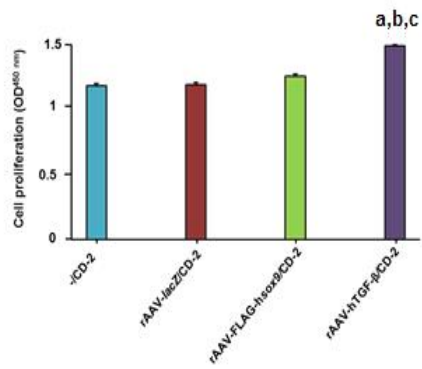
After 21 days, delivery of either rAAV-FLAG-hsox9 or rAAV-hTGF- $\beta$  in hMSCs via CD-2 resulted in significantly higher levels of glycosaminoglycans than all other conditions (1.3- and 1.2-fold difference using rAAV-FLAG-hsox9/CD-2 *versus* -/CD-2 and rAAV-*lacZ*/CD-2, respectively, always  $P \leq 0.002$ ; 1.8- and 1.7-fold difference using rAAV-hTGF- $\beta$ /CD-2 *versus* -/CD-2 and rAAV-*lacZ*/CD-2, respectively, always  $P \leq 0.001$ ), with TGF- $\beta$  having a stronger effect than SOX9 (1.4-fold difference;  $P \leq 0.001$ ) (**Figure 15B**).

After 21 days, delivery of either rAAV-FLAG-hsox9 or rAAV-hTGF- $\beta$  to hMSCs via CD-2 resulted in significantly higher levels of type-II collagen expression than all other conditions (17.8- and 15.4-fold difference using rAAV-FLAG-hsox9/CD-2 *versus* -/CD-2 and rAAV-*lacZ*/CD-2, respectively, always  $P \leq 0.001$ ; 14.4- and 12.5-fold difference using rAAV-hTGF- $\beta$ /CD-2 *versus* -/CD-2 and rAAV-*lacZ*/CD-2, respectively, always  $P \leq 0.001$ ), with SOX9 having a stronger effect than TGF- $\beta$  (1.2-fold difference;  $P \leq 0.002$ ) (**Figure 15C** and **Table 12**).

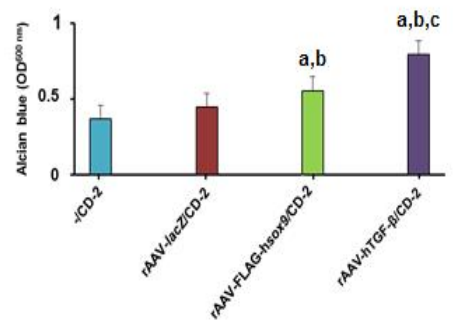
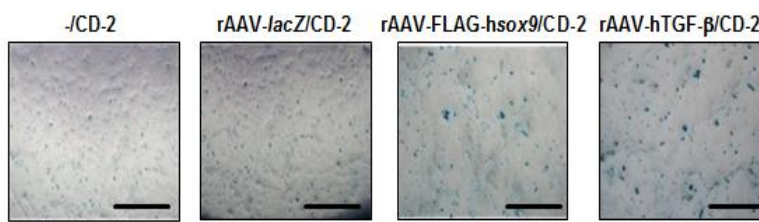
Interestingly, after 21 days, rAAV-FLAG-hsox9 or rAAV-hTGF- $\beta$  applied to hMSCs via CD-2 resulted in significantly lower levels of type-I collagen expression than all other conditions (20.1- and 20.2-fold difference using rAAV-FLAG-hsox9/CD-2 *versus* -/CD-2 and rAAV-*lacZ*/CD-2, respectively, always  $P \leq 0.001$ ; 22.7- and 22.9-fold difference using rAAV-hTGF- $\beta$ /CD-2 *versus* -/CD-2 and rAAV-*lacZ*/CD-2, respectively, always  $P \leq 0.001$ ), with no difference between SOX9 and TGF- $\beta$  ( $P = 0.319$ ) (**Figure 15D** and **Table 12**).

When type-X collagen expression was examined, similar results were observed (6.2- and 6.1-fold difference using rAAV-FLAG-hsox9/CD-2 *versus* -/CD-2 and rAAV-*lacZ*/CD-2, respectively, always  $P \leq 0.001$ ; 5.7-fold difference using rAAV-hTGF- $\beta$ /CD-2 *versus* -/CD-2 or rAAV-*lacZ*/CD-2, respectively, always  $P \leq 0.001$ ), with no differences between SOX9 and TGF- $\beta$  ( $P = 0.257$ ) (**Figure 15E** and **Table 12**).

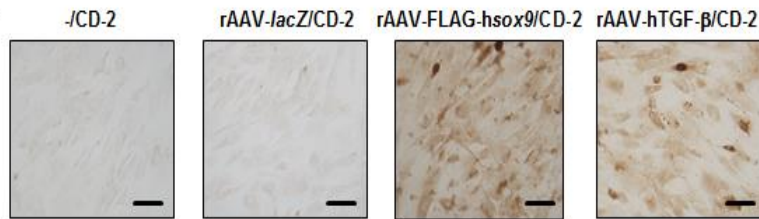
**A.**



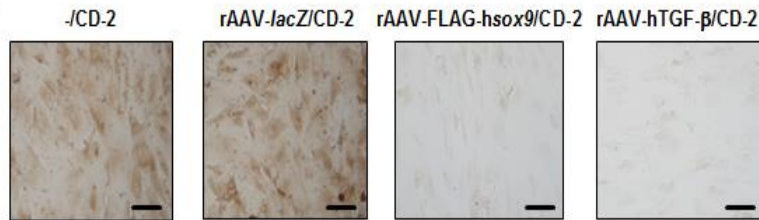
**B.**



**C.**



**D.**



**E.**

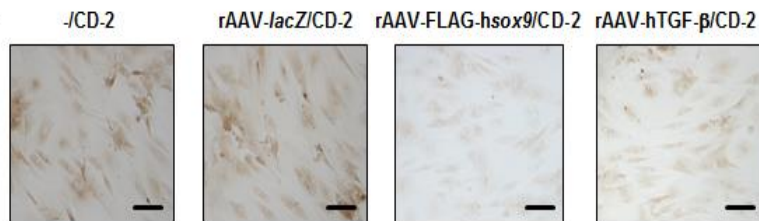


**Figure 15.** Biological activities in hMSCs transduced with rAAV/CD-2. The rAAV-FLAG-hsox9, rAAV-hTGF- $\beta$ , and rAAV-*lacZ* vectors (40  $\mu$ l each vector, i.e.  $8 \times 10^5$  transgene copies) were formulated with CD-2 (40  $\mu$ l) and the rAAV/carbon dot systems (80  $\mu$ l) were incubated with hMSCs (10,000 cells in 48-well plates; MOI = 80) for up to 21 days. Cell proliferation was examined using the Cell Proliferation Reagent WST-1 (**A**), glycosaminoglycans by alcian blue staining (light microscopy; magnification x4; scale bars: 200  $\mu$ m; representative data) with spectrophotometric analysis after solubilization (histograms) (**B**), and the deposition of type-II collagen (**C**), type-I collagen (**D**), and type-X collagen (**E**) by immunocytochemistry (magnification x20; scale bars: 50  $\mu$ m; representative data). rAAV-*lacZ*/CD-2 and CD-2 lacking rAAV were used as controls. Statistically significant relative to <sup>a</sup>-/CD-2, <sup>b</sup>rAAV-*lacZ*/CD-2, and <sup>c</sup>rAAV-FLAG-hsox9. Abbreviations: CD, carbon dot; rAAV, recombinant adeno-associated viral vector; *sox9*, sex-determining region Y-type high mobility group box 9 (cDNA); TGF- $\beta$ , transforming growth factor beta (cDNA). Image from (Meng et al., 2020).

## 8. DISCUSSION

Biomaterial-guided gene delivery using clinically adapted rAAV vectors (Cucchiarini, 2016; Cucchiarini and Madry, 2019; Díaz-Rodríguez et al., 2015; Lee et al., 2011; Madry et al., 2020a; Rey-Rico et al., 2015b, 2015c, 2016, 2017a, 2017b, 2018; Venkatesan et al., 2020a) is a novel, potent approach to treat focal cartilage lesions with non-invasive transfer and overexpression of chondroregenerative factors.

In the present study, we investigated the feasibility of delivering separate rAAV constructs coding for the highly chondroreparative SOX9 transcription factor (Bi et al., 1999) and TGF- $\beta$  growth factor (Johnstone et al., 1998; Mackay et al., 1998) to hMSCs via carbon dots as a means of stimulating biological activities in these cells, which are an advantageous source of progenitor cells for enhancing intrinsic healing processes in cartilage damage sites (Johnstone et al., 1998; Mackay et al., 1998; Pittenger et al., 1999).

The first hypothesis of our study was that carbon dots are potent systems to efficiently vectorize and release rAAV vectors, allowing for an optimal targeting and genetic modification of hMSCs via rAAV gene transfer. The findings of the present study confirm, for the first time to our best knowledge, that carbon dots are effective systems to successfully formulate and release rAAV gene transfer vectors.

The second hypothesis of the study was that optimal carbon dots can effectively deliver therapeutic (SOX9, TGF- $\beta$ ) rAAV vectors to reparative hMSCs as a novel, off-the-shelf system for cartilage repair. The findings of the present study shows that, among all the carbon dots tested, CD-2, a carbonaceous nanoparticle prepared by pyrolysis at normal pressure of a mixture of citric acid, PEG monomethyl ether 550 Da, and allowed for the highest intracellular vector release with a good over time maintenance for at least 10 days, the longest time point examined.

## **8.1. Carbon dots as effective systems to formulate and release rAAV gene transfer vectors**

We evaluated the ability of the carbon dots to deliver rAAV vectors to target hMSCs in a monolayer culture environment over time. The effective detection of live fluorescence in the samples after 24 hours compared with the control conditions (carbon dots formulating unlabeled rAAV and carbon dots lacking rAAV) showed good formulation of Cy3-labeled rAAV vectors with the different carbon dots, with no visible difference between carbon dots or when using Cy3-labeled rAAV vectors in the absence of carbon dot formulation. Compared with the other carbon dots (rAAV-*lacZ*/CD-1, rAAV-*lacZ*/CD-3, and rAAV-*lacZ*/CD-4) and free vector controls, CD-2 allowed for the most early vector release and excellent vector concentration maintenance over time (rAAV-*lacZ*/CD-2). For the first time, the current findings show that carbon dots can be used to effectively formulate and release rAAV gene transfer vectors. CD-2, a carbonaceous nanoparticle prepared by pyrolysis at normal pressure of a mixture of citric acid, PEG monomethyl ether 550 Da, and *N,N*-dimethylethylenediamine, allowed for the highest intracellular vector release with good over time maintenance for at least 10 days, the longest time point examined, among all the carbon dots tested here. These data suggest that the carbon dots increased the vector stability and may also favor vector diffusion, leading to the detection of higher amounts of rAAV capsids over time.

## **8.2. Effects of rAAV/carbon dot application on the viability of hMSCs**

The WST-1 assay revealed that the rAAV/CD-1 or rAAV/CD-2 systems were safe, with 100% cell viability on day 1 and no substantial differences compared with the corresponding control conditions (-, -/CD-1, -CD-2, and free vector administration). CD-3 and CD-4, on the other hand, had a substantial negative impact on cell viability (< 32%). On day 10, similar findings were made, with 100% viability using CD-1 and CD-2 in the corresponding control conditions and around 25-30% viability using CD-3 or CD-4. Most importantly, when used to deliver a reporter (rAAV-*lacZ*) gene vector to hMSCs for at least 10 days (up to 2.2-fold increase in *lacZ* expression relative to free vector treatment) in a safe manner (100% cell viability, presumably due to the presence of the

PEG protective shield around the particles), CD-2 was able to promote effective and sustained modification of hMSCs, reaching levels similar to those noted with other nanosized systems for rAAV delivery in hMSCs (Rey-Rico et al., 2015b). Compared with free vector administration and other control conditions, genetic alteration of hMSCs using CD-3 or CD-4 resulted in lower cell viability, whereas CD-1 resulted in lower gene transfer performance. This is the first data available showing that defined CD-2 can efficiently and durably target primary hMSCs via the potent rAAV vectors, without affecting the viability of the cells (100% over a period of 10 days).

### **8.3. CD-2 as an optimal carbon dot system to deliver therapeutic (SOX9, TGF- $\beta$ ) rAAV vectors**

The findings indicate that the optimal CD-2 nanoparticles could also improve the delivery of rAAV vectors coding for the therapeutic SOX9 and TGF- $\beta$  candidate genes in hMSCs, resulting in substantial overexpression of each transgene in the cells for a longer period of time (about 97.5% SOX9<sup>+</sup> cells using rAAV-FLAG-hsox9/CD-2 and 79.8% TGF- $\beta$ <sup>+</sup> cells with rAAV-hTGF- $\beta$ /CD-2 after 21 days) than control treatments ( $\leq$  7.8% and  $\leq$  11.8% transgene-expressing cells in the -/CD-2 and rAAV-*lacZ*/CD-2 conditions, respectively), as seen with free rAAV SOX9 or TGF- $\beta$  gene transfer (Frisch et al., 2014; Venkatesan et al., 2012). The TGF- $\beta$  levels produced by rAAV-hTGF- $\beta$ /CD-2 (155-225 pg/ml) were 4- to 56-fold higher than those produced by free rAAV-hTGF- $\beta$  gene transfer (17-24 pg/ml) (Frisch et al., 2014), most likely owing to the different vector doses used (MOI = 80-133 here compared with MOI = 4-20 using free vector gene administration, i.e. a 4- to 33-fold difference). Interestingly, the application of rAAV-hTGF- $\beta$ /CD-2 resulted in the detection of 52.8% SOX9<sup>+</sup> cells, likely due to an upregulation of SOX9 expression in response to TGF- $\beta$  production through rAAV/CD-2, as previously observed when using TGF- $\beta$  in its recombinant form (rTGF- $\beta$ ) (Murphy et al., 2015) or upon free rAAV-hTGF- $\beta$  gene transfer (Frisch et al., 2014), while no effects of SOX9 overexpression were seen on the levels of TGF- $\beta$ .

Effective SOX9 and TGF- $\beta$  overexpression via CD-2-guided gene delivery led to increased levels of cartilage matrix production in the cells (glycosaminoglycans, type-II

collagen expression) over time (21 days) relative to the control conditions, concordant with the respective pro-anabolic activities of SOX9 (Bi et al., 1999) and TGF- $\beta$  (Johnstone et al., 1998; Mackay et al., 1998; Pittenger et al., 1999), with observations showing short-term effects only of nonviral SOX9 gene transfer using arginine-based carbon dots (14 days) (Cao et al., 2018), and with our previous findings using free rAAV SOX9 or TGF- $\beta$  gene transfer (Frisch et al., 2014; Venkatesan et al., 2012).

Furthermore, rAAV-hTGF- $\beta$ /CD-2 application had a significant impact on hMSC proliferation, which is consistent with the properties of the growth factor (Mackay et al., 1998) and our previous findings using free rAAV TGF- $\beta$  gene transfer (Frisch et al., 2014). rAAV-FLAG-hsox9/CD-2, on the other hand, had no effect on this mechanism, in line with the activities of SOX9 (Akiyama et al., 2004) and with our findings from free rAAV SOX9 gene transfer (Venkatesan et al., 2012).

Interestingly, CD-2-guided delivery of either rAAV-FLAG-hsox9 or rAAV-hTGF- $\beta$  advantageously prevented the deposition of type-I and -X collagen in hMSCs over time compared with control treatments, which is consistent with the effects of SOX9 (Akiyama et al., 2004) and with results obtained using free rAAV SOX9 gene transfer (Venkatesan et al., 2012), but in contrast to findings using rTGF- $\beta$  (Johnstone et al., 1998) or upon free rAAV-hTGF- $\beta$  gene delivery (Frisch et al., 2014). This might be due to differences in culture conditions and cell environment (monolayer hMSC cultures here *versus* three-dimensional hMSC cultures in free rAAV-hTGF- $\beta$  gene transfer setting) (Frisch et al., 2014), or to differences in TGF- $\beta$  levels achieved through rAAV-hTGF- $\beta$ /CD-2 (155-225 pg/ml) and the amounts of rTGF- $\beta$  applied elsewhere (10 ng/ml, i.e. a 44- to 65-fold difference) (Johnstone et al., 1998).

Overall, the present work reports the possibility of transferring therapeutic rAAV (SOX9 or TGF- $\beta$ ) gene vectors to reparative hMSCs using optimal carbon-based nanoparticles as a novel, off-the-shelf system for cartilage repair. Analyses are ongoing to test the value of the approach in a three-dimensional environment (high density cultures) using single and combined CD-2-assisted rAAV SOX9/TGF- $\beta$  gene transfer to potentiate the effects of the two factors on cell proliferation (TGF- $\beta$ ) and matrix

deposition (glycosaminoglycans with TGF- $\beta$  superiority and type-II collagen with SOX9 superiority) (Scioli et al., 2017) and next in an orthotopic *in vivo* model of cartilage defect (Gentile and Garcovich, 2019; Im et al., 2011; Needham et al., 2014; Tao et al., 2016). Alternatively, concomitant SOX9 and TGF- $\beta$  gene transfer via rAAV (Tao et al., 2016) and CD-2 may be attempted to further increase the therapeutic outcomes obtained here. The current evaluation provides original evidence on the ability of carbon dot-guided therapeutic rAAV gene transfer in regenerative hMSCs as platforms for therapy of cartilage defects in translational protocols.

#### **8.4. Limitations and strengths**

The present study has some limitations. First, the current study did not evaluate the morphology of the carbon dots after combining them with rAAV. Cao *et al.* (Cao et al., 2018) revealed that positively charge carbon dot solution can combine negatively charge plasmid DNA solution to form nanoparticles. The nanoparticle size ratio reduced from 3:1 to 9:1 (carbon dot:plasmid DNA) due to the charge neutralization, bridging and aggregation of those two solutions. Further studies will need to include an evaluation of the morphology of rAAV/carbon dot systems by transmission electron microscopy and dynamical light scattering. Second, although the result of  $\zeta$  potential tests revealed that the carbon dots produced here had a positive charge (**Table 11**), we did not test the charge of rAAV/carbon dot complexes. Cao *et al.* (Cao et al., 2018) reported that the positive charge of carbon dot/plasmid DNA nanoparticles would facilitate a cellular uptake of carbon dot/plasmid DNA nanoparticles. The study however holds critical strengths. For the first time to the best of our knowledge, it demonstrates the potential of carbon dot-guided therapeutic rAAV gene delivery in hMSCs to trigger cartilage reparative cellular activities *in vitro*. It also provides evidence of the adapted use of CD-2 as an optimized vehicle for rAAV delivery in chondroregenerative hMSCs. Our ongoing work also shows the ability of CD-2 to deliver reparative SOX9 and TGF- $\beta$  sequences via rAAV vectors to human osteoarthritic articular chondrocytes in the goal of remodeling the altered cellular phenotype noted in these cells in human patients with OA (Meng et al., 2021).

## 8.5. Clinical implications

Biomaterial-guided delivery of chondrogenic gene sequences via gene transfer vectors to sites of cartilage injury is an appealing way to enhance cartilage repair by regulating their release in a better spatiotemporal manner while preserving gene transfer efficacy in a natural microenvironment (Cucchiarini and Madry, 2019). The present results advanced our general knowledge on the feasibility of using carbon dots for cartilage research (Meng et al., 2020). More research is however required to confirm the advantage of using carbon dots as convenient, adaptable, and effective treatments for cartilage defects as translation of biomaterial-mediated gene therapy in human clinical practice remains a significant challenge at the moment. First, more studies *in vitro* like those performed here (Meng et al., 2021) and in our previous investigations (Frisch et al., 2014; Rey-Rico et al., 2015a, 2016, 2017b; Venkatesan et al., 2020b, 2021) may define optimal conditions for effective therapy (presence, source, type, and dose of reparative cells, and/or gene vector). Second, experiments in clinically relevant animal models of cartilage defects may be performed as designed by our group (Madry et al., 2020a; Maihöfer et al., 2021) to evidence optimal carbon dot-based materials combined with effective rAAV gene vectors *in vivo*. It will be also particularly important to strictly compare carbon dot-guided gene therapy with biomaterial-free gene transfer and placebo in such investigations *in vivo* to show any improved performance of the composite system *versus* classical gene therapy. From a clinical standpoint, these data may result in the development of clinical trials applying carbon dot-based materials combined with effective rAAV gene vectors for articular cartilage repair.

## 9. CONCLUSIONS

Strategies based on the use of a variety of easily available biomaterials that have been modified for cartilage repair may be useful in supporting and enhancing the reparative activities in damaged cartilage (Cucchiari and Madry, 2019). Biocompatible and bioresorbable materials that are capable of (1) supporting cell growth and differentiation, (2) providing an adapted mechanical environment, and (3) allowing for the transport of cell nutrients are critically necessary to achieve these goals (Cucchiari and Madry, 2019). Gene therapy associated with the application of such biomaterials has a strong potential to improve the current therapeutic approaches for cartilage repair by providing off-the-shelf tools for the convenient treatment of cartilage lesions relative to scaffold-free gene transfer (Cucchiari and Madry, 2019). Carbon dots offer simple systems to deliver gene transfer vectors, being more compatible and tunable than solid scaffolds (Venkatesan et al., 2020b). The current work is the first study to report novel and highly biocompatible carbon dots as gene carriers to transfer SOX9 and TGF- $\beta$  sequences in hMSCs in an attempt to enhance the chondrogenic activities of these reparative cells. Among the nanoparticles tested here, CD-2 showed an optimal ability for rAAV delivery in hMSCs. Administration of therapeutic (SOX9, TGF- $\beta$ ) rAAV vectors in such cells via CD-2 led to the effective overexpression of each independent transgene, promoting enhanced cell proliferation (TGF- $\beta$ ) and cartilage matrix deposition (glycosaminoglycans, type-II collagen) for at least 21 days relative to control treatments. The present findings show the potential of combining hMSCs and gene-based approaches by administration of therapeutic rAAV gene transfer vectors to interactively stimulate chondroreparative activities of progenitor cells as a means to improve the processes controlling cartilage repair upon future implantation in sites of cartilage injuries. This work has strong value for the application of scaffold-guided gene therapy in cartilage tissue engineering *in vivo* in the future and may be combined with injectable approaches (Meng et al., 2019).

## 10. REFERENCES

- Akiyama H, Lyons JP, Mori-Akiyama Y, Yang X, Zhang R, Zhang Z, et al. (2004) Interactions between Sox9 and beta-catenin control chondrocyte differentiation. *Genes Dev* 18:1072-1087
- Akiyama H, Lefebvre V (2011) Unraveling the transcriptional regulatory machinery in chondrogenesis. *J Bone Miner Metab* 29:390-395
- Alvarez-Rivera F, Rey-Rico A, Venkatesan JK, Diaz-Gomez L, Cucchiaroni M, Concheiro A, et al. (2020) Controlled release of rAAV vectors from APMA-functionalized contact lenses for corneal gene therapy. *Pharmaceutics* 12:335
- Amano K, Hata K, Muramatsu S, Wakabayashi M, Takigawa Y, Ono K, et al. (2011) Arid5a cooperates with Sox9 to stimulate chondrocyte-specific transcription. *Mol Biol Cell* 22:1300-1311
- Appleton CT, Usmani SE, Bernier SM, Aigner T, Beier F (2007) Transforming growth factor alpha suppression of articular chondrocyte phenotype and Sox9 expression in a rat model of osteoarthritis. *Arthritis Rheum* 56:3693-3705
- Baker SN, Baker GA (2010) Luminescent carbon nanodots: emergent nanolights. *Angew Chem Int Ed Engl* 49:6726-6744
- Barter MJ, Gomez R, Hyatt S, Cheung K, Skelton AJ, Xu Y, et al. (2017) The long non-coding RNA ROCR contributes to SOX9 expression and chondrogenic differentiation of human mesenchymal stem cells. *Development* 144:4510-4521
- Bellamy N, Buchanan WW, Goldsmith CH, Campbell J, Stitt LW (1988) Validation study of WOMAC: a health status instrument for measuring clinically important patient relevant outcomes to antirheumatic drug therapy in patients with osteoarthritis of the hip or knee. *J Rheumatol* 15:1833-1840
- Berendsen AD, Olsen BR (2015) Bone development. *Bone* 80:14-18
- Bernard P, Harley VR (2010) Acquisition of SOX transcription factor specificity through protein-protein interaction, modulation of Wnt signalling and post-translational modification. *Int J Biochem Cell Biol* 42:400-410

- Bernstein P, Dong M, Graupner S, Corbeil D, Gelinsky M, Gunther KP, et al. (2009) Sox9 expression of alginate-encapsulated chondrocytes is stimulated by low cell density. *J Biomed Mater Res A* 91:910-918
- Bi W, Deng JM, Zhang Z, Behringer RR, de Crombrughe B (1999) Sox9 is required for cartilage formation. *Nat Genet* 22:85-89
- Blaney Davidson EN, Vitters EL, van der Kraan PM, van den Berg WB (2006) Expression of transforming growth factor-beta (TGFbeta) and the TGFbeta signalling molecule SMAD-2P in spontaneous and instability-induced osteoarthritis: role in cartilage degradation, chondrogenesis and osteophyte formation. *Ann Rheum Dis* 65:1414-1421
- Blaney Davidson EN, Remst DF, Vitters EL, van Beuningen HM, Blom AB, Goumans MJ, et al. (2009) Increase in ALK1/ALK5 ratio as a cause for elevated MMP-13 expression in osteoarthritis in humans and mice. *J Immunol* 182:7937-7945
- Bonnelye E, Zirngibl RA, Jurdic P, Aubin JE (2007) The orphan nuclear estrogen receptor-related receptor-alpha regulates cartilage formation in vitro: implication of Sox9. *Endocrinology* 148:1195-1205
- Bono N, Ponti F, Mantovani D, Candiani G (2020) Non-viral in vitro gene delivery: it is now time to set the bar! *Pharmaceutics* 12:183
- Buckwalter J, Mankin H (1997) Articular cartilage: degeneration and osteoarthritis, repair, regeneration, and transplantation. *Instr Course Lect* 47:487-504
- Buckwalter J, Mankin H (1998) Articular cartilage: tissue design and chondrocyte-matrix interactions. *Instr Course Lect* 47:477-486
- Burrage PS, Mix KS, Brinckerhoff CE (2006) Matrix metalloproteinases: role in arthritis. *Front Biosci* 11:529-543
- Buttgereit F, Burmester GR, Bijlsma JW (2015) Non-surgical management of knee osteoarthritis: where are we now and where do we need to go? *RMD Open* 1:e000027
- Cao L, Yang F, Liu G, Yu D, Li H, Fan Q, et al. (2011) The promotion of cartilage defect repair using adenovirus mediated Sox9 gene transfer of rabbit bone marrow mesenchymal stem cells. *Biomaterials* 32:3910-3920

- Cao X, Wang J, Deng W, Chen J, Wang Y, Zhou J, et al. (2018) Photoluminescent cationic carbon dots as efficient non-viral delivery of plasmid SOX9 and chondrogenesis of fibroblasts. *Sci Rep* 8:7057
- Chang T, Xie J, Li H, Li D, Liu P, Hu Y (2016) MicroRNA-30a promotes extracellular matrix degradation in articular cartilage via downregulation of Sox9. *Cell Prolif* 49:207-218
- Chen HC, Chang YH, Chuang CK, Lin CY, Sung LY, Wang YH, et al. (2009) The repair of osteochondral defects using baculovirus-mediated gene transfer with de-differentiated chondrocytes in bioreactor culture. *Biomaterials* 30:674-681
- Chen CG, Thuillier D, Chin EN, Alliston T (2012) Chondrocyte-intrinsic Smad3 represses Runx2-inducible matrix metalloproteinase 13 expression to maintain articular cartilage and prevent osteoarthritis. *Arthritis Rheum* 64:3278-3289
- Coricor G, Serra R (2016) TGF-beta regulates phosphorylation and stabilization of Sox9 protein in chondrocytes through p38 and Smad dependent mechanisms. *Sci Rep* 6:38616
- Cucchiari M, Madry H (2010) Genetic modification of mesenchymal stem cells for cartilage repair. *Biomed Mater Eng* 20:135-143
- Cucchiari M, Ekici M, Schetting S, Kohn D, Madry H (2011) Metabolic activities and chondrogenic differentiation of human mesenchymal stem cells following recombinant adeno-associated virus-mediated gene transfer and overexpression of fibroblast growth factor 2. *Tissue Eng Part A* 17:1921-1933
- Cucchiari M, Orth P, Madry H (2013) Direct rAAV SOX9 administration for durable articular cartilage repair with delayed terminal differentiation and hypertrophy in vivo. *J Mol Med (Berl)* 91:625-636
- Cucchiari M, Madry H (2014) Overexpression of human IGF-I via direct rAAV-mediated gene transfer improves the early repair of articular cartilage defects in vivo. *Gene Ther* 21:811-819
- Cucchiari M, Henrionnet C, Mainard D, Pinzano A, Madry H (2015) New trends in articular cartilage repair. *J Exp Orthop* 2:8
- Cucchiari M (2016) Human gene therapy: novel approaches to improve the current gene delivery systems. *Discov Med* 21:495-506

- Cucchiarini M, Rey-Rico A. Controlled gene delivery systems for articular cartilage repair. *Advances in Biomaterials for Biomedical Applications*. Springer 2017:261-300
- Cucchiarini M, Asen AK, Goebel L, Venkatesan JK, Schmitt G, Zurakowski D, et al. (2018) Effects of TGF-beta overexpression via rAAV gene transfer on the early repair processes in an osteochondral defect model in minipigs. *Am J Sports Med* 46:1987-1996
- Cucchiarini M, Madry H (2019) Biomaterial-guided delivery of gene vectors for targeted articular cartilage repair. *Nat Rev Rheumatol* 15:18-29
- Díaz-Rodríguez P, Rey-Rico A, Madry H, Landin M, Cucchiarini M (2015) Effective genetic modification and differentiation of hMSCs upon controlled release of rAAV vectors using alginate/poloxamer composite systems. *Int J Pharm* 496:614-626
- Ding H, Du F, Liu P, Chen Z, Shen J (2015) DNA-carbon dots function as fluorescent vehicles for drug delivery. *ACS Appl Mater Interfaces* 7:6889-6897
- Dy P, Wang W, Bhattaram P, Wang Q, Wang L, Ballock RT, et al. (2012) Sox9 directs hypertrophic maturation and blocks osteoblast differentiation of growth plate chondrocytes. *Dev Cell* 22:597-609
- Fan J, Claudel M, Ronzani C, Arezki Y, Lebeau L, Pons F (2019) Physicochemical characteristics that affect carbon dot safety: lessons from a comprehensive study on a nanoparticle library. *Int J Pharm* 569:118521
- Feng L, Yang ZM, Li YC, Wang HX, Lo JHT, Zhang XT, et al. (2021) Linc-ROR promotes mesenchymal stem cells chondrogenesis and cartilage formation via regulating SOX9 expression. *Osteoarthritis Cartilage* 29:568-578
- Flotte TR, Carter BJ (1995) Adeno-associated virus vectors for gene therapy. *Gene Ther* 2:357-362
- Flotte TR (2000) Size does matter: overcoming the adeno-associated virus packaging limit. *Respir Res* 1:16-18
- Frisch J, Venkatesan JK, Rey-Rico A, Schmitt G, Madry H, Cucchiarini M (2014) Determination of the chondrogenic differentiation processes in human bone marrow-derived mesenchymal stem cells genetically modified to overexpress transforming growth factor-beta via recombinant adeno-associated viral vectors. *Hum Gene Ther* 25:1050-1060

- Frisch J, Rey-Rico A, Venkatesan JK, Schmitt G, Madry H, Cucchiari M (2016) TGF-beta gene transfer and overexpression via rAAV vectors stimulates chondrogenic events in human bone marrow aspirates. *J Cell Mol Med* 20:430-440
- Gao L, Sheu TJ, Dong Y, Hoak DM, Zuscik MJ, Schwarz EM, et al. (2013) TAK1 regulates SOX9 expression in chondrocytes and is essential for postnatal development of the growth plate and articular cartilages. *J Cell Sci* 126:5704-5713
- Gao L, Goebel LKH, Orth P, Cucchiari M, Madry H (2018) Subchondral drilling for articular cartilage repair: a systematic review of translational research. *Dis Model Mech* 11:dmm034280
- Garza-Veloz I, Romero-Diaz VJ, Martinez-Fierro ML, Marino-Martinez IA, Gonzalez-Rodriguez M, Martinez-Rodriguez HG, et al. (2013) Analyses of chondrogenic induction of adipose mesenchymal stem cells by combined co-stimulation mediated by adenoviral gene transfer. *Arthritis Res Ther* 15:R80
- Gelse K, von der Mark K, Aigner T, Park J, Schneider H (2003) Articular cartilage repair by gene therapy using growth factor-producing mesenchymal cells. *Arthritis Rheum* 48:430-441
- Gelse K, Muhle C, Knaup K, Swoboda B, Wiesener M, Hennig F, et al. (2008) Chondrogenic differentiation of growth factor-stimulated precursor cells in cartilage repair tissue is associated with increased HIF-1alpha activity. *Osteoarthritis Cartilage* 16:1457-1465
- Gentile P, Garcovich S (2019) Concise review: adipose-derived stem cells (ASCs) and adipocyte-secreted exosomal microRNA (A-SE-miR) modulate cancer growth and promote wound repair. *J Clin Med* 8:855
- Glass KA, Link JM, Brunger JM, Moutos FT, Gersbach CA, Guilak F (2014) Tissue-engineered cartilage with inducible and tunable immunomodulatory properties. *Biomaterials* 35:5921-5931
- Goormer RS, Maris TM, Gelberman R, Boyer M, Silva M, Amiel D (2000) Nonviral in vivo gene therapy for tissue engineering of articular cartilage and tendon repair. *Clin Orthop Relat Res* 379 Suppl:S189-S200

- Grande DA, Schwartz JA, Brandel E, Chahine NO, Sgaglione N (2013) Articular cartilage repair: where we have been, where we are now, and where we are headed. *Cartilage* 4:281-285
- Grieger JC, Samulski RJ (2012) Adeno-associated virus vectorology, manufacturing, and clinical applications. *Methods Enzymol* 507:229-254
- Grimm D, Kay MA (2003) From virus evolution to vector revolution: use of naturally occurring serotypes of adeno-associated virus (AAV) as novel vectors for human gene therapy. *Curr Gene Ther* 3:281-304
- Gruber HE, Ingram J, Norton HJ, Wei LY, Frausto A, Mills BG, et al. (2004) Alterations in growth plate and articular cartilage morphology are associated with reduced SOX9 localization in the magnesium-deficient rat. *Biotech Histochem* 79:45-52
- Gu S, Boyer TG, Naski MC (2012) Basic helix-loop-helix transcription factor Twist1 inhibits transactivator function of master chondrogenic regulator Sox9. *J Biol Chem* 287:21082-21092
- Hattori T, Muller C, Gebhard S, Bauer E, Pausch F, Schlund B, et al. (2010) SOX9 is a major negative regulator of cartilage vascularization, bone marrow formation and endochondral ossification. *Development* 137:901-911
- Haudenschild DR, Chen J, Pang N, Lotz MK, D'Lima DD (2010) Rho kinase-dependent activation of SOX9 in chondrocytes. *Arthritis Rheum* 62:191-200
- He X, Ohba S, Hojo H, McMahon AP (2016) AP-1 family members act with Sox9 to promote chondrocyte hypertrophy. *Development* 143:3012-3023
- Hu L, Sun Y, Li S, Wang X, Hu K, Wang L, et al. (2014) Multifunctional carbon dots with high quantum yield for imaging and gene delivery. *Carbon* 67:508-513
- Huang W, Zhou X, Lefebvre V, de Crombrughe B (2000) Phosphorylation of SOX9 by cyclic AMP-dependent protein kinase A enhances SOX9's ability to transactivate a Col2a1 chondrocyte-specific enhancer. *Mol Cell Biol* 20:4149-4158
- Huskisson EC (1974) Measurement of pain. *Lancet* 2:1127-1131
- Hussain S, Sun M, Guo Y, Mushtaq N, Zhao Y, Yuan Y, et al. (2018) SFMBT2 positively regulates SOX9 and chondrocyte proliferation. *Int J Mol Med* 42:3503-3512
- Ibraheem D, Elaissari A, Fessi H (2014) Gene therapy and DNA delivery systems. *Int J Pharm* 459:70-83

- Ikeda T, Kamekura S, Mabuchi A, Kou I, Seki S, Takato T, et al. (2004) The combination of SOX5, SOX6, and SOX9 (the SOX trio) provides signals sufficient for induction of permanent cartilage. *Arthritis Rheum* 50:3561-3573
- Ikegami D, Akiyama H, Suzuki A, Nakamura T, Nakano T, Yoshikawa H, et al. (2011) Sox9 sustains chondrocyte survival and hypertrophy in part through Pik3ca-Akt pathways. *Development* 138:1507-1519
- Im GI, Kim HJ, Lee JH (2011) Chondrogenesis of adipose stem cells in a porous PLGA scaffold impregnated with plasmid DNA containing SOX trio (SOX-5,-6 and -9) genes. *Biomaterials* 32:4385-4392
- Ivkovic A, Pascher A, Hudetz D, Maticic D, Jelic M, Dickinson S, et al. (2010) Articular cartilage repair by genetically modified bone marrow aspirate in sheep. *Gene Ther* 17:779-789
- Jacques C, Recklies AD, Levy A, Berenbaum F (2007) HC-gp39 contributes to chondrocyte differentiation by inducing SOX9 and type II collagen expressions. *Osteoarthritis Cartilage* 15:138-146
- Janssen JN, Batschkus S, Schimmel S, Bode C, Schminke B, Miosge N (2019) The Influence of TGF-beta3, EGF, and BGN on SOX9 and RUNX2 expression in human chondrogenic progenitor cells. *J Histochem Cytochem* 67:117-127
- Johnstone B, Hering TM, Caplan AI, Goldberg VM, Yoo JU (1998) In vitro chondrogenesis of bone marrow-derived mesenchymal progenitor cells. *Exp Cell Res* 238:265-272
- Kailasa SK, Bhamore JR, Koduru JR, Park TJ (2019) Carbon dots as carriers for the development of controlled drug and gene delivery systems. *Biomed Appl Nanoparticles*:295-317
- Kawakami Y, Tsuda M, Takahashi S, Taniguchi N, Esteban CR, Zemmyo M, et al. (2005) Transcriptional coactivator PGC-1alpha regulates chondrogenesis via association with Sox9. *Proc Natl Acad Sci U S A* 102:2414-2419
- Kawamura K, Chu CR, Sobajima S, Robbins PD, Fu FH, Izzo NJ, et al. (2005) Adenoviral-mediated transfer of TGF-beta1 but not IGF-1 induces chondrogenic differentiation of human mesenchymal stem cells in pellet cultures. *Exp Hematol* 33:865-872

- Kellgren J, Lawrence J (1957) Radiological assessment of osteo-arthrosis. *Ann Rheum Dis* 16:494
- Kim J, Park J, Kim H, Singha K, Kim WJ (2013) Transfection and intracellular trafficking properties of carbon dot-gold nanoparticle molecular assembly conjugated with PEI-pDNA. *Biomaterials* 34:7168-7180
- Kim J, Lin B, Kim S, Choi B, Evseenko D, Lee M (2015) TGF-beta1 conjugated chitosan collagen hydrogels induce chondrogenic differentiation of human synovium-derived stem cells. *J Biol Eng* 9:1
- Kim S, Han S, Kim Y, Kim HS, Gu YR, Kang D, et al. (2019) Tankyrase inhibition preserves osteoarthritic cartilage by coordinating cartilage matrix anabolism via effects on SOX9 PARylation. *Nat Commun* 10:4898
- Ko JY, Sun YC, Li WC, Wang FS (2016) Chaperonin 60 regulation of SOX9 ubiquitination mitigates the development of knee osteoarthritis. *J Mol Med (Berl)* 94:755-769
- Kozhemyakina E, Lassar AB, Zelzer E (2015) A pathway to bone: signaling molecules and transcription factors involved in chondrocyte development and maturation. *Development* 142:817-831
- Kupcsik L, Stoddart MJ, Li Z, Benneker LM, Alini M (2010) Improving chondrogenesis: potential and limitations of SOX9 gene transfer and mechanical stimulation for cartilage tissue engineering. *Tissue Eng Part A* 16:1845-1855
- Kypriotou M, Fossard-Demoor M, Chadjichristos C, Ghayor C, de Crombrughe B, Pujol JP, et al. (2003) SOX9 exerts a bifunctional effect on type II collagen gene (COL2A1) expression in chondrocytes depending on the differentiation state. *DNA Cell Biol* 22:119-129
- Las Heras F, Gahunia HK, Pritzker KP (2012) Articular cartilage development: a molecular perspective. *Orthop Clin North Am* 43:155-171
- Lee HJ, Lee JS, Chansakul T, Yu C, Elisseeff JH, Yu SM (2006) Collagen mimetic peptide-conjugated photopolymerizable PEG hydrogel. *Biomaterials* 27:5268-5276
- Lee HH, Haleem AM, Yao V, Li J, Xiao X, Chu CR (2011) Release of bioactive adeno-associated virus from fibrin scaffolds: effects of fibrin glue concentrations. *Tissue Eng Part A* 17:1969-1978

- Lefebvre V, Behringer RR, de Crombrughe B (2001) L-Sox5, Sox6 and Sox9 control essential steps of the chondrocyte differentiation pathway. *Osteoarthritis Cartilage* 9 Suppl A:S69-S75
- Lefebvre V, Dvir-Ginzberg M (2017) SOX9 and the many facets of its regulation in the chondrocyte lineage. *Connect Tissue Res* 58:2-14
- Li TF, Gao L, Sheu TJ, Sampson ER, Flick LM, Konttinen YT, et al. (2010) Aberrant hypertrophy in Smad3-deficient murine chondrocytes is rescued by restoring transforming growth factor beta-activated kinase 1/activating transcription factor 2 signaling: a potential clinical implication for osteoarthritis. *Arthritis Rheum* 62:2359-2369
- Li H, Kang Z, Liu Y, Lee S-T (2012) Carbon nanodots: synthesis, properties and applications. *J Mater Chem* 22:24230-24253
- Li J, Dong S (2016) The signaling pathways involved in chondrocyte differentiation and hypertrophic differentiation. *Stem Cells Int* 2016:2470351
- Lin H, Cheng AW, Alexander PG, Beck AM, Tuan RS (2014) Cartilage tissue engineering application of injectable gelatin hydrogel with in situ visible-light-activated gelation capability in both air and aqueous solution. *Tissue Eng Part A* 20:2402-2411
- Liu CJ, Zhang Y, Xu K, Parsons D, Alfonso D, Di Cesare PE (2007) Transcriptional activation of cartilage oligomeric matrix protein by Sox9, Sox5, and Sox6 transcription factors and CBP/p300 coactivators. *Front Biosci* 12:3899-3910
- Liu TM, Guo XM, Tan HS, Hui JH, Lim B, Lee EH (2011) Zinc-finger protein 145, acting as an upstream regulator of SOX9, improves the differentiation potential of human mesenchymal stem cells for cartilage regeneration and repair. *Arthritis Rheum* 63:2711-2720
- Liu C, Zhang P, Zhai X, Tian F, Li W, Yang J, et al. (2012) Nano-carrier for gene delivery and bioimaging based on carbon dots with PEI-passivation enhanced fluorescence. *Biomaterials* 33:3604-3613
- Liu CF, Samsa WE, Zhou G, Lefebvre V (2017) Transcriptional control of chondrocyte specification and differentiation. *Semin Cell Dev Biol* 62:34-49

- Mackay AM, Beck SC, Murphy JM, Barry FP, Chichester CO, Pittenger MF (1998) Chondrogenic differentiation of cultured human mesenchymal stem cells from marrow. *Tissue Eng* 4:415-428
- Madry H, Cucchiari M, Terwilliger EF, Trippel SB (2003) Recombinant adeno-associated virus vectors efficiently and persistently transduce chondrocytes in normal and osteoarthritic human articular cartilage. *Hum Gene Ther* 14:393-402
- Madry H\*, Gao L\*, Rey-Rico A, Venkatesan JK, Muller-Brandt K, Cai X, et al. (2020a) Thermosensitive hydrogel based on PEO-PPO-PEO poloxamers for a controlled in situ release of recombinant adeno-associated viral vectors for effective gene therapy of cartilage defects. *Adv Mater* 32:e1906508 (\*shared authorship)
- Madry H, Venkatesan JK, Carballo-Pedrares N, Rey-Rico A, Cucchiari M (2020b) Scaffold-mediated gene delivery for osteochondral repair. *Pharmaceutics* 12:930
- Maihöfer J\*, Madry H\*, Rey-Rico A, Venkatesan JK, Goebel L, Schmitt G, et al. (2021) Hydrogel-guided, rAAV-mediated IGF-I overexpression enables long-term cartilage repair and protection against perifocal osteoarthritis in a large-animal full-thickness chondral defect model at one year in vivo. *Adv Mater* 33:e2008451 (\*shared authorship)
- Makihira S, Yan W, Ohno S, Kawamoto T, Fujimoto K, Okimura A, et al. (1999) Enhancement of cell adhesion and spreading by a cartilage-specific noncollagenous protein, cartilage matrix protein (CMP/Matrilin-1), via integrin alpha1beta1. *J Biol Chem* 274:11417-11423
- Mansfield JC, Mandalia V, Toms A, Winlove CP, Brasselet S (2019) Collagen reorganization in cartilage under strain probed by polarization sensitive second harmonic generation microscopy. *J R Soc Interface* 16:20180611
- Mao G, Xu Y, Long D, Yan K (2021) Exosome-transported circRNA\_0001236 enhances chondrogenesis and suppresses cartilage degradation via MIR-3677-3P/SOX9 pathway. *Osteoarthritis Cartilage* 29:S296
- Martel-Pelletier J, Boileau C, Pelletier JP, Roughley PJ (2008) Cartilage in normal and osteoarthritis conditions. *Best Pract Res Clin Rheumatol* 22:351-384

- Martinez-Sanchez A, Dudek KA, Murphy CL (2012) Regulation of human chondrocyte function through direct inhibition of cartilage master regulator SOX9 by microRNA-145 (miRNA-145). *J Biol Chem* 287:916-924
- Martinez-Sanchez A, Murphy CL (2013) miR-1247 functions by targeting cartilage transcription factor SOX9. *J Biol Chem* 288:30802-30814
- Mbita Z, Hull R, Dlamini Z (2014) Human immunodeficiency virus-1 (HIV-1)-mediated apoptosis: new therapeutic targets. *Viruses* 6:3181-3227
- Meng W, Gao L, Venkatesan JK, Wang G, Madry H, Cucchiari M (2019) Translational applications of photopolymerizable hydrogels for cartilage repair. *J Exp Orthop* 6:47
- Meng W, Rey-Rico A, Claudel M, Schmitt G, Speicher-Mentges S, Pons F, et al. (2020) rAAV-mediated overexpression of SOX9 and TGF-beta via carbon dot-guided vector delivery enhances the biological activities in human bone marrow-derived mesenchymal stromal cells. *Nanomaterials (Basel)* 10:855
- Meng W, Venkatesan J, Rey-Rico A, Schmitt G, Speicher-Mentges S, Pons F, et al. (2021) Carbon dot-guided delivery of therapeutic (SOX9, TGF- $\beta$ ) rAAV vectors to enhance the biological activity of human articular chondrocytes. *Osteoarthritis Cartilage* 29:S206-S207
- Mitchell PG, Magna HA, Reeves LM, Lopresti-Morrow LL, Yocum SA, Rosner PJ, et al. (1996) Cloning, expression, and type II collagenolytic activity of matrix metalloproteinase-13 from human osteoarthritic cartilage. *J Clin Invest* 97:761-768
- Monahan PE, Samulski RJ (2000) AAV vectors: is clinical success on the horizon? *Gene Ther* 7:24-30
- Murphy JM, Fink DJ, Hunziker EB, Barry FP (2003) Stem cell therapy in a caprine model of osteoarthritis. *Arthritis Rheum* 48:3464-3474
- Murphy MK, Huey DJ, Hu JC, Athanasiou KA (2015) TGF-beta1, GDF-5, and BMP-2 stimulation induces chondrogenesis in expanded human articular chondrocytes and marrow-derived stromal cells. *Stem Cells* 33:762-773
- Nam HY, Park JH, Kim K, Kwon IC, Jeong SY (2009) Lipid-based emulsion system as non-viral gene carriers. *Arch Pharm Res* 32:639-646

- Needham CJ, Shah SR, Dahlin RL, Kinard LA, Lam J, Watson BM, et al. (2014) Osteochondral tissue regeneration through polymeric delivery of DNA encoding for the SOX trio and RUNX2. *Acta Biomater* 10:4103-4112
- Newman AP (1998) Articular cartilage repair. *Am J Sports Med* 26:309-324
- Nishimura R, Hata K, Takahata Y, Murakami T, Nakamura E, Yagi H (2017) Regulation of cartilage development and diseases by transcription factors. *J Bone Metab* 24:147-153
- Nishimura R, Hata K, Nakamura E, Murakami T, Takahata Y (2018) Transcriptional network systems in cartilage development and disease. *Histochem Cell Biol* 149:353-363
- Oliveira Silva M, Gregory JL, Ansari N, Stok KS (2020) Molecular signaling interactions and transport at the osteochondral interface: a review. *Front Cell Dev Biol* 8:750
- Peppers MJ, Milner PI, Tew SR, Clegg PD (2010) Regulation of SOX9 in normal and osteoarthritic equine articular chondrocytes by hyperosmotic loading. *Osteoarthritis Cartilage* 18:1502-1508
- Piera-Velazquez S, Hawkins DF, Whitecavage MK, Colter DC, Stokes DG, Jimenez SA (2007) Regulation of the human SOX9 promoter by Sp1 and CREB. *Exp Cell Res* 313:1069-1079
- Pierrat P, Wang R, Kereselidze D, Lux M, Didier P, Kichler A, et al. (2015) Efficient in vitro and in vivo pulmonary delivery of nucleic acid by carbon dot-based nanocarriers. *Biomaterials* 51:290-302
- Pittenger MF, Mackay AM, Beck SC, Jaiswal RK, Douglas R, Mosca JD, et al. (1999) Multilineage potential of adult human mesenchymal stem cells. *Science* 284:143-147
- Podsakoff G, Wong KK, Jr., Chatterjee S (1994) Efficient gene transfer into nondividing cells by adeno-associated virus-based vectors. *J Virol* 68:5656-5666
- Rai R, Alwani S, Badea I (2019) Polymeric nanoparticles in gene therapy: new avenues of design and optimization for delivery applications. *Polymers (Basel)* 11:745
- Remst DF, Blaney Davidson EN, Vitters EL, Bank RA, van den Berg WB, van der Kraan PM (2014) TGF- $\beta$  induces lysyl hydroxylase 2b in human synovial osteoarthritic fibroblasts through ALK5 signaling. *Cell Tissue Res* 355:163-171

- Retting KN, Song B, Yoon BS, Lyons KM (2009) BMP canonical Smad signaling through Smad1 and Smad5 is required for endochondral bone formation. *Development* 136:1093-1104
- Rey-Rico A, Frisch J, Venkatesan JK, Schmitt G, Madry H, Cucchiarini M (2015a) Determination of effective rAAV-mediated gene transfer conditions to support chondrogenic differentiation processes in human primary bone marrow aspirates. *Gene Ther* 22:50-57
- Rey-Rico A, Venkatesan JK, Frisch J, Rial-Hermida I, Schmitt G, Concheiro A, et al. (2015b) PEO-PPO-PEO micelles as effective rAAV-mediated gene delivery systems to target human mesenchymal stem cells without altering their differentiation potency. *Acta Biomater* 27:42-52
- Rey-Rico A, Venkatesan JK, Frisch J, Schmitt G, Monge-Marcet A, Lopez-Chicon P, et al. (2015c) Effective and durable genetic modification of human mesenchymal stem cells via controlled release of rAAV vectors from self-assembling peptide hydrogels with a maintained differentiation potency. *Acta Biomater* 18:118-127
- Rey-Rico A, Cucchiarini M (2016a) Controlled release strategies for rAAV-mediated gene delivery. *Acta Biomater* 29:1-10
- Rey-Rico A, Cucchiarini M (2016b) Recent tissue engineering-based advances for effective rAAV-mediated gene transfer in the musculoskeletal system. *Bioengineered* 7:175-188
- Rey-Rico A, Frisch J, Venkatesan JK, Schmitt G, Rial-Hermida I, Taboada P, et al. (2016) PEO-PPO-PEO carriers for rAAV-mediated transduction of human articular chondrocytes in vitro and in a human osteochondral defect model. *ACS Appl Mater Interfaces* 8:20600-20613
- Rey-Rico A, Babicz H, Madry H, Concheiro A, Alvarez-Lorenzo C, Cucchiarini M (2017a) Supramolecular polypseudorotaxane gels for controlled delivery of rAAV vectors in human mesenchymal stem cells for regenerative medicine. *Int J Pharm* 531:492-503
- Rey-Rico A, Venkatesan JK, Schmitt G, Concheiro A, Madry H, Alvarez-Lorenzo C, et al. (2017b) rAAV-mediated overexpression of TGF-beta via vector delivery in polymeric micelles stimulates the biological and reparative activities of human

articular chondrocytes in vitro and in a human osteochondral defect model. *Int J Nanomedicine* 12:6985-6996

Rey-Rico A, Venkatesan JK, Schmitt G, Speicher-Mentges S, Madry H, Cucchiari M (2018) Effective remodelling of human osteoarthritic cartilage by sox9 gene transfer and overexpression upon delivery of rAAV vectors in polymeric micelles. *Mol Pharm* 15:2816-2826

Rezaee M, Oskuee RK, Nassirli H, Malaekheh-Nikouei B (2016) Progress in the development of lipopolyplexes as efficient non-viral gene delivery systems. *J Control Release* 236:1-14

Robbins PD, Ghivizzani SC (1998) Viral vectors for gene therapy. *Pharmacol Ther* 80:35-47

Robbins PD, Tahara H, Ghivizzani SC (1998) Viral vectors for gene therapy. *Trends Biotechnol* 16:35-40

Robins JC, Akeno N, Mukherjee A, Dalal RR, Aronow BJ, Koopman P, et al. (2005) Hypoxia induces chondrocyte-specific gene expression in mesenchymal cells in association with transcriptional activation of Sox9. *Bone* 37:313-322

Samulski RJ, Berns KI, Tan M, Muzyczka N (1982) Cloning of adeno-associated virus into pBR322: rescue of intact virus from the recombinant plasmid in human cells. *Proc Natl Acad Sci U S A* 79:2077-2081

Samulski RJ, Chang LS, Shenk T (1987) A recombinant plasmid from which an infectious adeno-associated virus genome can be excised in vitro and its use to study viral replication. *J Virol* 61:3096-3101

Samulski RJ, Chang LS, Shenk T (1989) Helper-free stocks of recombinant adeno-associated viruses: normal integration does not require viral gene expression. *J Virol* 63:3822-3828

Scioli MG, Bielli A, Gentile P, Cervelli V, Orlandi A (2017) Combined treatment with platelet-rich plasma and insulin favours chondrogenic and osteogenic differentiation of human adipose-derived stem cells in three-dimensional collagen scaffolds. *J Tissue Eng Regen Med* 11:2398-2410

- Sekiya I, Tsuji K, Koopman P, Watanabe H, Yamada Y, Shinomiya K, et al. (2000) SOX9 enhances aggrecan gene promoter/enhancer activity and is up-regulated by retinoic acid in a cartilage-derived cell line, TC6. *J Biol Chem* 275:10738-10744
- Sekiya I, Koopman P, Tsuji K, Mertin S, Harley V, Yamada Y, et al. (2001) Dexamethasone enhances SOX9 expression in chondrocytes. *J Endocrinol* 169:573-579
- Serra R, Johnson M, Filvaroff EH, LaBorde J, Sheehan DM, Derynck R, et al. (1997) Expression of a truncated, kinase-defective TGF-beta type II receptor in mouse skeletal tissue promotes terminal chondrocyte differentiation and osteoarthritis. *J Cell Biol* 139:541-552
- Shakibaei M, Seifarth C, John T, Rahmanzadeh M, Mobasheri A (2006) Igf-I extends the chondrogenic potential of human articular chondrocytes in vitro: molecular association between Sox9 and Erk1/2. *Biochem Pharmacol* 72:1382-1395
- Sharma B, Williams CG, Khan M, Manson P, Elisseeff JH (2007) In vivo chondrogenesis of mesenchymal stem cells in a photopolymerized hydrogel. *Plast Reconstr Surg* 119:112-120
- Shen J, Li J, Wang B, Jin H, Wang M, Zhang Y, et al. (2013) Deletion of the transforming growth factor beta receptor type II gene in articular chondrocytes leads to a progressive osteoarthritis-like phenotype in mice. *Arthritis Rheum* 65:3107-3119
- Shi C, Zheng W, Wang J (2021) lncRNA-CRNDE regulates BMSC chondrogenic differentiation and promotes cartilage repair in osteoarthritis through SIRT1/SOX9. *Mol Cell Biochem* 476:1881-1890
- Simon TM, Jackson DW (2018) Articular cartilage: injury pathways and treatment options. *Sports Med Arthrosc Rev* 26:31-39
- Song H, Park KH (2020) Regulation and function of SOX9 during cartilage development and regeneration. *Semin Cancer Biol* 67:12-23
- Steadman JR, Rodkey WG, Rodrigo JJ (2001) Microfracture: surgical technique and rehabilitation to treat chondral defects. *Clin Orthop Relat Res* 391 Suppl:S362-S369

- Steinert AF, Weissenberger M, Kunz M, Gilbert F, Ghivizzani SC, Gobel S, et al. (2012) Indian hedgehog gene transfer is a chondrogenic inducer of human mesenchymal stem cells. *Arthritis Res Ther* 14:R168
- Sum CH, Shortall SM, Wong S, Wettig SD (2018) Non-viral gene delivery. *Exp Suppl* 110:3-68
- Sun L, Li J, Xiao X (2000) Overcoming adeno-associated virus vector size limitation through viral DNA heterodimerization. *Nat Med* 6:599-602
- Symon A, Harley V (2017) SOX9: a genomic view of tissue specific expression and action. *Int J Biochem Cell Biol* 87:18-22
- Takahashi I, Nuckolls GH, Takahashi K, Tanaka O, Semba I, Dashner R, et al. (1998) Compressive force promotes sox9, type II collagen and aggrecan and inhibits IL-1beta expression resulting in chondrogenesis in mouse embryonic limb bud mesenchymal cells. *J Cell Sci* 111 (Pt 14):2067-2076
- Tao K, Frisch J, Rey-Rico A, Venkatesan JK, Schmitt G, Madry H, et al. (2016) Co-overexpression of TGF-beta and SOX9 via rAAV gene transfer modulates the metabolic and chondrogenic activities of human bone marrow-derived mesenchymal stem cells. *Stem Cell Res Ther* 7:20
- Thielen NGM, van der Kraan PM, van Caam APM (2019) TGFbeta/BMP signaling pathway in cartilage homeostasis. *Cells* 8:969
- Thomas CE, Ehrhardt A, Kay MA (2003) Progress and problems with the use of viral vectors for gene therapy. *Nat Rev Genet* 4:346-358
- Tsuda M, Takahashi S, Takahashi Y, Asahara H (2003) Transcriptional co-activators CREB-binding protein and p300 regulate chondrocyte-specific gene expression via association with Sox9. *J Biol Chem* 278:27224-27229
- Ulrich-Vinther M, Duch MR, Soballe K, O'Keefe RJ, Schwarz EM, Pedersen FS (2004) In vivo gene delivery to articular chondrocytes mediated by an adeno-associated virus vector. *J Orthop Res* 22:726-734
- Ushita M, Saito T, Ikeda T, Yano F, Higashikawa A, Ogata N, et al. (2009) Transcriptional induction of SOX9 by NF-kappaB family member RelA in chondrogenic cells. *Osteoarthritis Cartilage* 17:1065-1075

- van der Kraan PM (2017) The changing role of TGFbeta in healthy, ageing and osteoarthritic joints. *Nat Rev Rheumatol* 13:155-163
- Venkatesan JK, Ekici M, Madry H, Schmitt G, Kohn D, Cucchiari M (2012) SOX9 gene transfer via safe, stable, replication-defective recombinant adeno-associated virus vectors as a novel, powerful tool to enhance the chondrogenic potential of human mesenchymal stem cells. *Stem Cell Res Ther* 3:22
- Venkatesan JK, Falentin-Daudre C, Leroux A, Migonney V, Cucchiari M (2020a) Biomaterial-guided recombinant adeno-associated virus delivery from poly(sodium styrene sulfonate)-grafted poly(epsilon-caprolactone) films to target human bone marrow aspirates. *Tissue Eng Part A* 26:450-459
- Venkatesan JK, Meng W, Rey-Rico A, Schmitt G, Speicher-Mentges S, Falentin-Daudre C, et al. (2020b) Enhanced chondrogenic differentiation activities in human bone marrow aspirates via sox9 overexpression mediated by pNaSS-grafted PCL film-guided rAAV gene transfer. *Pharmaceutics* 12:280
- Venkatesan JK, Cai X, Meng W, Rey-Rico A, Schmitt G, Speicher-Mentges S, et al. (2021) pNaSS-grafted PCL film-guided rAAV TGF-beta gene therapy activates the chondrogenic activities in human bone marrow aspirates. *Hum Gene Ther* doi: 10.1089/hum.2020.32
- Verschure PJ, Joosten LA, van der Kraan PM, Van den Berg WB (1994) Responsiveness of articular cartilage from normal and inflamed mouse knee joints to various growth factors. *Ann Rheum Dis* 53:455-460
- Vincenti MP, Coon CI, Mengshol JA, Yocum S, Mitchell P, Brinckerhoff CE (1998) Cloning of the gene for interstitial collagenase-3 (matrix metalloproteinase-13) from rabbit synovial fibroblasts: differential expression with collagenase-1 (matrix metalloproteinase-1). *Biochem J* 331 (Pt 1):341-346
- Vincenti MP, Brinckerhoff CE (2001) Early response genes induced in chondrocytes stimulated with the inflammatory cytokine interleukin-1beta. *Arthritis Res* 3:381-388
- Wang X, Li Y, Han R, He C, Wang G, Wang J, et al. (2014) Demineralized bone matrix combined bone marrow mesenchymal stem cells, bone morphogenetic protein-2 and transforming growth factor-beta3 gene promoted pig cartilage defect repair. *PLoS One* 9:e116061

- Wang Z, Liang DC, Bai JY, Kang N, Feng JY, Yang ZQ (2015) Overexpression of Sox9 gene by the lentiviral vector in rabbit bone marrow mesenchymal stem cells for promoting the repair of cartilage defect. *Zhongguo Gu Shang* 28:433-440
- Wang Q, Tan QY, Xu W, Qi HB, Chen D, Zhou S, et al. (2017) Cartilage-specific deletion of Alk5 gene results in a progressive osteoarthritis-like phenotype in mice. *Osteoarthritis Cartilage* 25:1868-1879
- Weissenberger M, Weissenberger MH, Gilbert F, Groll J, Evans CH, Steinert AF (2020) Reduced hypertrophy in vitro after chondrogenic differentiation of adult human mesenchymal stem cells following adenoviral SOX9 gene delivery. *BMC Musculoskelet Disord* 21:109
- Whyte WA, Orlando DA, Hnisz D, Abraham BJ, Lin CY, Kagey MH, et al. (2013) Master transcription factors and mediator establish super-enhancers at key cell identity genes. *Cell* 153:307-319
- Williams CG, Kim TK, Taboas A, Malik A, Manson P, Elisseff J (2003) In vitro chondrogenesis of bone marrow-derived mesenchymal stem cells in a photopolymerizing hydrogel. *Tissue Eng* 9:679-688
- Wojdasiewicz P, Poniatowski LA, Szukiewicz D (2014) The role of inflammatory and anti-inflammatory cytokines in the pathogenesis of osteoarthritis. *Mediators Inflamm* 2014:561459
- Wong LY, Xia B, Wolvetang E, Cooper-White J (2018) Targeted, stimuli-responsive delivery of plasmid DNA and miRNAs using a facile self-assembled supramolecular nanoparticle Ssystem. *Biomacromolecules* 19:353-363
- Wu Z, Asokan A, Samulski RJ (2006) Adeno-associated virus serotypes: vector toolkit for human gene therapy. *Mol Ther* 14:316-327
- Wu Q, Kim KO, Sampson ER, Chen D, Awad H, O'Brien T, et al. (2008) Induction of an osteoarthritis-like phenotype and degradation of phosphorylated Smad3 by Smurf2 in transgenic mice. *Arthritis Rheum* 58:3132-3144
- Wu Y, Li J, Kong Y, Chen D, Liu B, Wang W (2013) HSV-1 based vector mediated IL-1 $\alpha$  gene for knee osteoarthritis in rabbits. *Zhong Nan Da Xue Xue Bao Yi Xue Ban* 38:590-596

- Wu YF, Wu HC, Kuan CH, Lin CJ, Wang LW, Chang CW, et al. (2016) Multi-functionalized carbon dots as theranostic nanoagent for gene delivery in lung cancer therapy. *Sci Rep* 6:21170
- Xu X, Ray R, Gu Y, Ploehn HJ, Gearheart L, Raker K, et al. (2004) Electrophoretic analysis and purification of fluorescent single-walled carbon nanotube fragments. *J Am Chem Soc* 126:12736-12737
- Yan Z, Zhang Y, Duan D, Engelhardt JF (2000) Trans-splicing vectors expand the utility of adeno-associated virus for gene therapy. *Proc Natl Acad Sci U S A* 97:6716-6721
- Yang X, Chen L, Xu X, Li C, Huang C, Deng CX (2001) TGF-beta/Smad3 signals repress chondrocyte hypertrophic differentiation and are required for maintaining articular cartilage. *J Cell Biol* 153:35-46
- Yoo JU, Barthel TS, Nishimura K, Solchaga L, Caplan AI, Goldberg VM, et al. (1998) The chondrogenic potential of human bone-marrow-derived mesenchymal progenitor cells. *J Bone Joint Surg Am* 80:1745-1757
- Yoo JU, Mandell I, Angele P, Johnstone B (2000) Chondrogenitor cells and gene therapy. *Clin Orthop Relat Res* 379 Suppl:S164-S170
- Zhang HT, Yang J, Liang GH, Gao XJ, Sang Y, Gui T, et al. (2017) Andrographolide induces cell cycle arrest and apoptosis of chondrosarcoma by targeting TCF-1/SOX9 axis. *J Cell Biochem* 118:4575-4586
- Zhang W, Cheng P, Hu W, Yin W, Guo F, Chen A, et al. (2018) Inhibition of microRNA-384-5p alleviates osteoarthritis through its effects on inhibiting apoptosis of cartilage cells via the NF-kappaB signaling pathway by targeting SOX9. *Cancer Gene Ther* 25:326-338
- Zhao Q, Eberspaecher H, Lefebvre V, De Crombrughe B (1997) Parallel expression of Sox9 and Col2a1 in cells undergoing chondrogenesis. *Dev Dyn* 209:377-386
- Zhou J, Deng W, Wang Y, Cao X, Chen J, Wang Q, et al. (2016a) Cationic carbon quantum dots derived from alginate for gene delivery: one-step synthesis and cellular uptake. *Acta Biomater* 42:209-219

- Zhou Z, Yu H, Wang Y, Guo Q, Wang L, Zhang H (2016b) ZNF606 interacts with Sox9 to regulate chondrocyte differentiation. *Biochem Biophys Res Commun* 479:920-926
- Zhou Y, Wang T, Hamilton JL, Chen D (2017) Wnt/beta-catenin signaling in osteoarthritis and in other forms of arthritis. *Curr Rheumatol Rep* 19:53
- Zhu H, Tang J, Tang M, Cai H (2013) Upregulation of SOX9 in osteosarcoma and its association with tumor progression and patients' prognosis. *Diagn Pathol* 8:183

## 11. PUBLICATIONS AND PRESENTATIONS

### 11.1. Publications

1. **W. Meng**, L. Gao, J.K. Venkatesan, G. Wang, H. Madry, M. Cucchiarini, Translational applications of photopolymerizable hydrogels for cartilage repair, *J Exp Orthop* 6(1) (2019) 47. Impact factor: currently in evaluation
2. **W. Meng**, A. Rey-Rico, M. Claudel, G. Schmitt, S. Speicher-Mentges, F. Pons, L. Lebeau, J.K. Venkatesan, M. Cucchiarini, rAAV-mediated overexpression of SOX9 and TGF-beta via carbon dot-guided vector delivery enhances the biological activities in human bone marrow-derived mesenchymal stromal cells, *Nanomaterials (Basel)* 10(5) (2020) 855. Impact factor: 4.324 (2020)
3. J.K. Venkatesan, **W. Meng**, A. Rey-Rico, G. Schmitt, S. Speicher-Mentges, C. Falentin-Daudre, A. Leroux, H. Madry, V. Migonney, M. Cucchiarini, Enhanced chondrogenic differentiation activities in human bone marrow aspirates via sox9 overexpression mediated by pNaSS-grafted PCL film-guided rAAV gene transfer, *Pharmaceutics* 12(3) (2020) 280. Impact factor: 4.421 (2020)
4. J.K. Venkatesan, X. Cai, **W. Meng**, A. Rey-Rico, G. Schmitt, S. Speicher-Mentges, C. Falentin-Daudre, A. Leroux, H. Madry, V. Migonney, M. Cucchiarini, pNaSS-grafted PCL film-guided rAAV TGF-beta gene therapy activates the chondrogenic activities in human bone marrow aspirates, *Hum Gene Ther* (2021) doi:10.1089/hum.2020.329. Impact factor: 4.510 (2021)
5. Maihöfer J\*, Madry H\*, Rey-Rico A, Venkatesan JK, Goebel L, Schmitt G, Speicher-Mentges S, Cai X, **Meng W**, Zurakowski D, Menger MD, Laschke MW, and Cucchiarini M. Hydrogel-guided, rAAV-mediated IGF-I overexpression enables long-term cartilage repair and protection against perifocal osteoarthritis in a large animal full-thickness chondral defect model at one year in vivo. *Adv Mater* (2021) e2008451 (\*shared authorship). Impact factor: 27.398 (2021)

## 11.2. Poster presentations

1. **W. Meng**, J.K. Venkatesan, A. Rey-Rico, G. Schmitt, F. Pons, L. Lebeau, H. Madry, M. Cucchiarini. Benefits of using carbon dot (MC148) for the effective delivery of rAAV vectors in human articular chondrocytes. *Orthopaedic Research Society 2021 Annual Meeting*, 02/2021.
2. **W. Meng**, J.K. Venkatesan, R. Beninatto, D. Galesso, G. Schmitt, S. Speicher-Mentges, H. Madry, M. Cucchiarini. Photopolymerizable hydrogel-guided delivery of rAAV vectors in human bone marrow-derived mesenchymal stromal cells. *Orthopaedic Research Society 2021 Annual Meeting*, 02/2021.

## 12. ACKNOWLEDGEMENTS

Throughout the preparation of this dissertation, I received a great deal of support and assistance. First and foremost, I would like to express my deep and sincere gratitude to my supervisor, Prof. Dr. rer. nat. Magali Cucchiarini Madry, and also to Prof. Dr. med. Henning Madry, whose expertise was invaluable in formulating the research questions and methodology. Their insightful feedback, continuous support, and persistent guidance pushed me to sharpen my thinking and brought my work to a higher level. Without their meticulous patience, valuable guidance, and selfless help throughout the whole project, this dissertation would not be possible. It is their kind help and patient support that have made my study and life in the Germany a wonderful time. It is a great privilege and honor to work and study under their guidance. I am extremely grateful for what they have offered me. Special thanks to Prof. Dr. med. Guanglin Wang and Prof. Dr. med. Zongke Zhou for their continuous encouragement throughout my years of study. They look forward to pursuing a wide range of international cooperative projects, in particular those promoting the mutual exchange of findings from basic biomedical research, clinical research and clinical application.

I would like to offer my special thanks to Dr. rer. nat. Jagadeesh K. Venkatesan for his treasured assistance at every step of the research project which was really influential in shaping my experiment methods. Many thanks to Dr. rer. nat. Liang Gao for the unreserved support of my work, for his immense knowledge and plentiful experience have encouraged me in all the time of my academic research. I am grateful for your friendly care.

I would also like to thank Ms. Gertrud Schmitt and Mrs. Susanne Speicher-Mentges for their technical support on my study. Special thanks to Dr. rer. nat. Ana Rey-Rico for her scientific guidance and invaluable suggestions for encouraging guidance during my academic research. I wish to show my gratitude to Dr. rer. nat. Mickaël Claudel, Prof. Dr.

rer. nat. Françoise Pons, and Prof. Dr. rer. nat. Luc Lebeau for providing excellent biomaterial systems to complete my research.

Special thanks to my best partner, Dr. Xiaoyu Cai, who always helped me with everything and made me never feel homesick. To all the current and former members of the Center of Experimental Orthopaedics, especially to Mrs. Sonja Ramin, Dr. rer. nat. Tamás Oláh, Dr. Wei Liu, Dr. rer. nat. Mahnaz Amini: many thanks to all of you for the nice working atmosphere, a cherished time spent together in the lab, and in social settings.

My gratitude extends to financial support from the China Scholarship Council for the funding opportunity to undertake my studies at the Center of Experimental Orthopaedics, Saarland University.

Finally, I wish to acknowledge the support and great love of my fiancée, Yang Bai; my parents; and my best friend, Huang Zhong. Without their tremendous understanding and encouragement in the past few years, it would be impossible for me to complete my studies.